Spring 5-31-2015

Experimental determination of the agitation requirements for solids suspension in dissolution systems using a mini paddle apparatus

Yang Song
New Jersey Institute of Technology

ABSTRACT

EXPERIMENTAL DETERMINATION OF THE AGITATION REQUIREMENTS FOR SOLIDS SUSPENSION IN DISSOLUTION SYSTEMS USING A MINI PADDLE APPARATUS

by
Yang Song

Dissolution testing is a critical step in quality control of manufactured final products in the pharmaceutical industry. The United State Pharmacopeia (USP) Dissolution Testing Apparatus 2 (paddle) is the most widely used dissolution test devices in the pharmaceutical industry to formulate solid drug dosage forms and to develop quality control specifications for its manufacturing process.

Mini vessels and mini paddle dissolution testing systems are smaller versions of the USP 2 Apparatus. The concept of the mini paddle apparatus is similar to that of the USP 2 setup but it is scaled down about to 1/5 of the volume and 40% with respect to vessel and impeller sizes. Mini vessel systems, requiring a small volume (200 mL) and a mini paddle impeller, are becoming increasing common in the pharmaceutical industry to overcome the limitations associated with the USP 2 dissolution testing method, especially for dissolution testing involving very small tablets. Mini apparatuses can be useful tools in characterizing drug release profiles since smaller sample sizes and smaller volumes of media are needed, thus offering several advantages in terms of substance, analytical, and material cost savings when evaluating release properties of drug candidates.

Despite their increasing importance in dissolution testing, little information is currently available on mini vessels, and especially on the agitation speed needed to prevent “coning” effects. Typically during dissolution testing, a disintegrating tablet becomes rapidly fragmented, and the resulting solid particles may or may not become

suspended depending on the agitation speed of the paddle and other geometric and operating parameters. "Coning" (the accumulation of particle fragments from a disintegrating tablet) often appears in dissolution testing but can be eliminated by increasing the agitation speed N. Therefore, it is important to be able to predict the minimum rotation speed at which coning phenomena disappears in a dissolution testing system and especially in mini vessels systems.

The focus of this work was the determination of the minimum agitation speed, N_{js}, at which the just suspended state by dispersed particles is achieved in a mini paddle system (thus removing "coning" effects). In the past, N_{js}, has been experimentally obtained in mixing systems by determining the agitation speed at which no particles are visually observed to be at rest on the vessel bottom for more than one to two seconds. Therefore, the first objective of this work was to develop an observer-independent method to measure experimentally N_{js}. This was achieved by extending to mini vessel a method that was recently developed in our laboratory and that is based on the determination of the fraction of unsuspended solids in the vessel at different agitation speed ($N_{js\text{-}Ds}$ method). The results of this method agree well the visually observable values of N_{js} ($N_{js\text{-}visual}$).

Once new method was validated in mini vessels, N_{js} was experimentally measured using well characterized solid particles under a number of operating conditions, such as liquid level-to-vessel diameter ratio (H/T), particle size (d_p), and paddle clearance-to-vessel diameter ratio C_b/T). The results could be interpreted using the Zwietering Equation originally developed for solids suspension in baffled stirred tanks. The Zwietering *"S"* parameter was obtained for the mini vessel system thus enabling the use of this equation to predict when "coning" effects can be eliminated in mini vessel systems during tablet dissolution testing.

EXPERIMENTAL DETERMINATION OF THE AGITATION REQUIREMENTS FOR SOLIDS SUSPENSION IN DISSOLUTION SYSTEMS USING A MINI PADDLE APPARATUS

by
Yang Song

A Thesis
Submitted to the Faculty of
New Jersey Institute of Technology
in Partial Fulfillment of the Requirements for the Degree of
Master of Science in Pharmaceutical Engineering

Otto H. York Department of Chemical, Biological and Pharmaceutical Engineering

May 2015

Blank Page

APPROVAL PAGE

EXPERIMENTAL DETERMINATION OF THE AGITATION REQUIREMENTS FOR SOLIDS SUSPENSION IN DISSOLUTION SYSTEMS USING A MINI PADDLE APPARATUS

Yang Song

Dr. Piero M. Armenante, Thesis Advisor Date
Distinguished Professor of Chemical, Biological and Pharmaceutical Engineering, NJIT

Dr. Laurent Simon, Committee Member Date
Associate Professor of Chemical, Biological and Pharmaceutical Engineering, NJIT

Gerard Bredael, Committee Member Date
Associate Principal Scientist, Merck Inc.

BIOGRAPHICAL SKETCH

Author: Yang Song

Degree: Master of Science

Date: May 3, 2015

Undergraduate and Graduate Education:

- Master of Science in Pharmaceutical Engineering,
  New Jersey Institute of Technology, Newark, NJ, 2015

- Bachelor of Since in Pharmacy,
  Guizhou Medical University, Guizhou, People Republic of China, 2007

Major: Pharmaceutical Engineering

< To my family >

ACKNOWLEDGMENT

I owe my gratitude to all those people who have made this thesis possible and because of whom my graduate experience has been one that I will cherish forever.

My deepest gratitude is to my advisor, Dr. Piero M. Armenante. I have been amazingly fortunate to have him as advisor since he gave me the freedom to explore on my own, and he provided me with kind guidance, helpful suggestions, encouragement that inspired confidence in me. His patience and support helped me overcome many crisis situations and helped me complete this thesis.

I would like to express my sincere thanks to Dr. Laurent Simon and Mr. Gerard Bredael, for their patience in reviewing the thesis, for their recommendations and everything.

I would also like to express my deepest gratitude towards Bing Wang, PhD student in mixing lab for supporting me at every stage of thesis and the kind and warm friendship you shared with me.

Finally, I would like to thank my parents, and my boyfriend Wenxiao for their patience, unconditional love, and encouragements. This work was not possible without their presence and support.

TABLE OF CONTENTS

TABLE OF CONTENTS
(Continued)

Chapter	Page

LIST OF TABLES

LIST OF FIGURES

LIST OF FIGURES
(Continued)

Figure **Page**

NOMENCLATURE

D	Impeller diameter (mm)
T	Mini vessel internal diameter (mm)
H	Liquid height (mm)
C_b	Bottom clearance (mm)
N	Rotational speed (rpm)
N_{js}	Minimum agitation speed for solid suspension
ν	Viscosity (m^2/s)
ρ_s	Density of particle (kg/m^3)
ρ_l	Density of particle (kg/m^3)
X	Solid fraction
d_p	Particle size (μm)

CHAPTER 1

INTRODUCTION

1.1 Background

Dissolution testing is a critical step in quality control of manufactured final products in the pharmaceutical industry, and it is one of the standard methods to assess batch-to-batch consistency of solid oral drug delivery systems, such as tablets and capsules. One of the most widely used dissolution test devices is the United State Pharmacopeia (USP) Apparatus 2 (paddle). Apparatus 2 and the method associated with it are useful in the pharmaceutical and biotechnology industry to formulate solid drug dosage forms and to develop quality control specifications for its manufacturing process.

Dissolution is an operation during which the solid particles decrease in size and ultimately disappears as they become incorporated into the liquid as a solute. Dissolution is a mass transfer-controlled process. The intensity of agitation plays a significant role on solid-liquid mass transfer and is often the rate-controlling step. To find out the solid states of suspension is the key for charactering the mixing system conditions. A standard compendia dissolution apparatus are the first choice for development of new dissolution methods. Nevertheless, limitations coming from the amount of material available, analytical sensitivity, lack of discrimination or bio relevance may warrant the use of non-compendia methods. In this regard, the use of small volume dissolution methods offers strong advantages.

Mini vessels and mini paddle dissolution testing systems are scaled down versions of the typical USP 2 apparatus used in routine dissolution testing. A smaller-volume vessel with scaled-down paddle can be useful to handle volumes capable of

Nano and pictogram levels of drug that have demanded more from traditional dissolution apparatus. The mini paddle apparatus has evolved as the method to achieve this purpose. The concept of the mini paddle apparatus arose from the USP-2 paddle setup but scaled down about to 1/5 of the volume and 40% with respect to the dimensions.

Mini apparatuses can be useful tools in characterizing drug release profiles since smaller sample sizes and smaller volumes of media are needed, thus offering several advantages in terms of substance, analytical, and material cost savings when evaluating release properties of drug candidates. Mini vessel systems requiring a small volume vessel (200 mL) and a mini paddle impeller are becoming increasing common in the pharmaceutical industry to overcome the limitations associated with the USP 2 drug dissolution testing method, especially for dissolution testing involving very small tablets.

Despite their increasing importance in dissolution testing, little information is currently available on mini vessels, and especially on the agitation speed needed to prevent "coning" effects. Typically during dissolution testing, a disintegrating tablet becomes rapidly fragmented, and the resulting solid particles may or may not become suspended depending on the agitation speed of the paddle and other geometric and operating parameters. "Coning" (the accumulation of particle fragments from a disintegrating tablet) often appears in dissolution testing but can be eliminated by increasing the agitation speed N. Therefore, it is important to be able to predict the minimum rotation speed at which coning phenomena disappears in a dissolution testing system.

In the mixing literature, the determination and prediction of the minimum agitation speed, N_{js}, at which the just suspended state is achieved by the particles dispersed in a liquid in a stirred system is a topic that has been studied for stirred tanks and reactors (Armenante and Uehara-Nagamine 1998). The reason for this is that mixing, suspension, and dispersion of solids in liquids are involved in about 80% of the operations in the chemical and pharmaceutical industries, including processes ranging from leaching and complete dissolution of reagents to suspension of catalysts and reaction products (such as precipitates and crystals). Solid suspension consists of lifting the solids initially settled on the vessel bottom to a desired level or suspension state (e.g., off-bottom, uniform). Dispersion of solids in a stirred liquid is the physical process in which the solids are dispersed by the action of an agitator in a fluid to achieve a partial or uniform dispersion state. In agitated vessels, the behavior of the solids suspension is generally classified into three levels: on-bottom motion, uniform suspension and complete off-bottom (Paul et al., 2004). When the agitation speed is gradually increased in a vessel filled initially with finely divided solids, some solids will begin to move and suspended until all solids are more homogeneous. It is often important to provide enough agitation to completely suspend the solids off the vessel bottom. Below this off-bottom particle suspension state, the total solid-liquid interfacial surface area is not completely or efficiently utilized. The particle suspension states as shown in Figure 1.1.

Although N_{js} has been obtained for a number of mixing systems for regular size dissolution system, very little information is available in the literature for the solid suspensions in the mini paddle system of interest here. Also, below this off-bottom point state, the total solid-liquid interfacial surface area is not completely utilized and the results obtained could have bias from person to person. The utilization of the mini paddle apparatus needs to provide accurate, data for quality and stability assurance during the formulation reached full-scale or scale-down production.

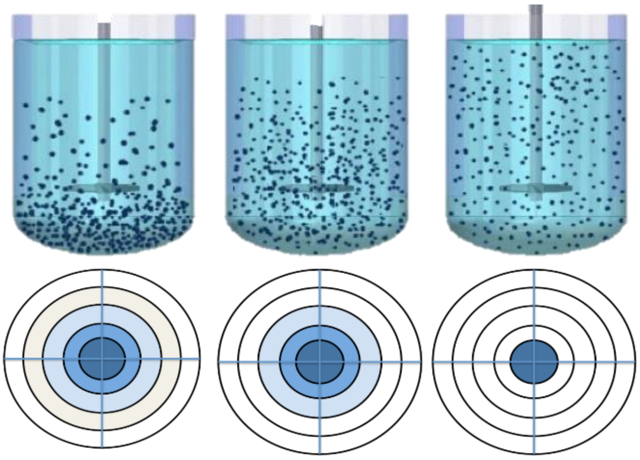

(a) (b) (c)

Figure 1.1 Degrees of suspension (a) Partial suspension (b) Complete suspension (c) Uniform suspension.

Therefore, to develop a new experimental method to determine objectively (i.e., independently of the observer) the minimum impeller speed N_{js} to just suspend solid particles in mini vessels and avoid coning is important for evaluating the dissolution testing using a mini paddle apparatus.

1.2 Objective of This Work

From the above discussion, it follows that it would be important to be able to determine the agitation speed, N_{js}, at which the just suspended state is achieved by dispersed particles in a mini paddle system. In the past, N_{js}, has been obtained experimentally by determining the agitation speed at which no particles are visually observed to be at rest on the vessel bottom for more than one to two seconds. However, the hydrodynamics in stirred vessels are complex and turbulent. The interplay between solid and liquid materials, vessel design, impeller type and location, and level of agitation all determine the efficiency of the mixing process. It would be advantageous to develop a new experimental method to determine objectively (i.e., independently of the observer) the minimum impeller speed N_{js} to just suspend solid particles in mini vessels and avoid coning.

Therefore, the first objective of this work was to develop such an observer-independent method to measure experimentally N_{js}. This was achieved here by extending to mini vessel a method that was recently developed in our laboratory and that is based on the determination of the fraction of unsuspended solids in the vessel at different agitation speed.

Once the first objective has been achieved, the second objective was to determine N_{js} in mini vessels for a variety of operating conditions, such as: *H/T*, d_p and C_b/T).

Finally another objective was to determine if available correlations for N_{js} such as the Zwietering Equation particles in baffled stirred vessels could also be used for mini vessels, and if so what the parameters in such equation would be.

CHAPTER 2

EXPERIMETNAL APPARATUS, MATERIALS, AND METHODS

2.1 Apparatus

The equipment and methods described in this section were used to obtain experimental results for the minimum agitation speed for complete solids suspension, N_{js} in a hemispherical-bottom mixing mini vessel provided with a mini impeller under different operation conditions.

2.1.1 Hemispherical-Bottom Dissolution Mini Vessel and Mini Impeller

A dissolution mini vessel and a mini paddle impeller, as shown in Figure 2.1 (a) were used as the agitation system. The vessel consisted of an un-baffled, cylindrical, transparent glass tank with a hemispherical bottom and an overall capacity of 200mL (Distek Inc., North Brunswick, New Jersey)

Circles and radii were drawn on the vessel bottom using a black mark pen in order to measure the portion of the vessel bottom covered by solids during solid suspension experiments, as shown in Figure 2.1 (b). When the vessel was filled with different volume of dissolution media, the corresponding liquid height, *H*, as measured and marked from the bottom of the vessel.

The agitation system consists of a mini paddle mounted on a shaft centrally located in the vessel and profiled to follow the hemispherical portion of the vessel. The basic dimensions of the mini vessel shown in Figure 2.2, measured with a caliper.

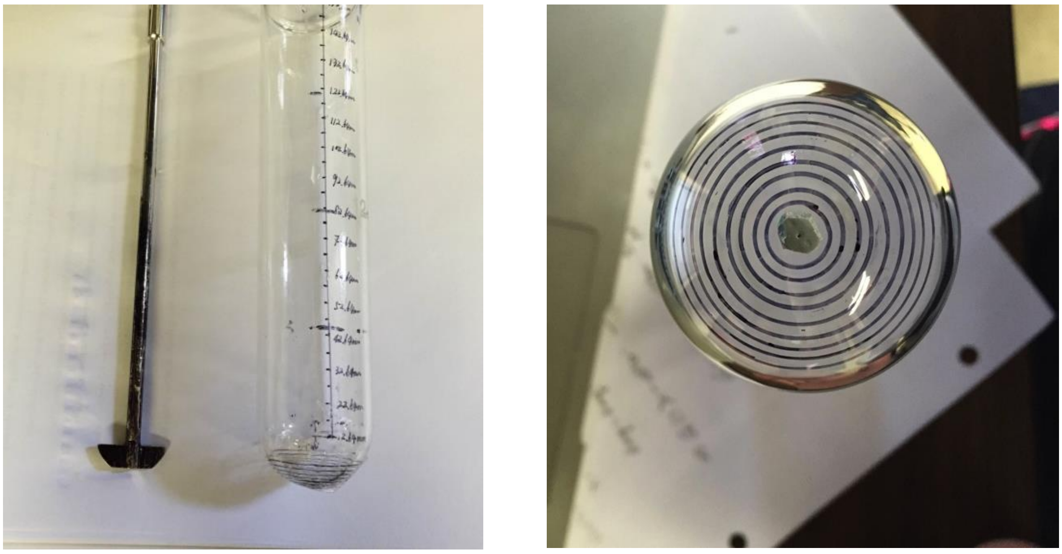

(a) (b)

Figure 2.1 (a) A hemispherical-bottomed mini vessel with mini paddle (b) Bottom view of the vessel with equally spaced circles drawn on its bottom.

- Internal diameter (T): 40.00mm
- Overall height: 175mm
- Height of dish bottom: 15mm
- Height of cylindrical section: 160mm
- Thickness of cylinder: 2.36mm

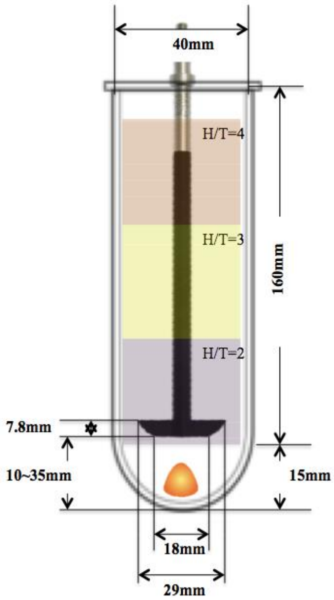

Figure 2.2 Dimensions of mini vessel.

The impeller consisted of a single-blade paddle impeller connected to the Distek system (Distek Inc.) motor with the steel shaft. The following are the impeller dimensions measured with a caliper, as shown in Figure 2.3(a). Compared to the regular impeller, the difference is shown in Figure 2.3(b), and details are shown in Table 2.1.

- Impeller diameter (D): 29mm
- Blade upper chord: 29mm
- Blade lower chord: 18mm
- Blade height: 7.5mm
- Blade thickness: 6.2mm

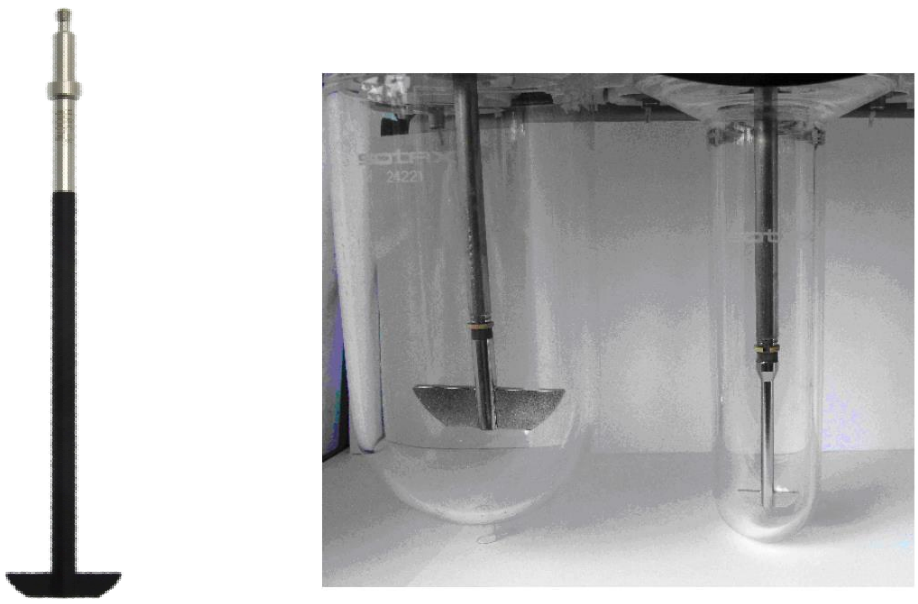

(a) (b)

Figure 2.3 (a) Impeller used in hemispherical-bottom small volume mixing system (b) Comparison between a USP 2 (1L) dissolution vessel and the mini vessel (right side).

Table 2.1 Dissolution-Difference in Dimension (mm) of the Small and USP Vessels and Paddles

	USP 2 1-Liter System	Mini Vessel System
Vessel		
Height	168±8	165
Internal Diameter	102±4	40
Paddle		
Blade Upper chord	74.0±0.5	29
Blade Lower chord	42.0±1.0	18
Height	19.0±1.0	7.8
Impeller clearance	25±2	10~35

Note: The impeller clearance measured from the bottom of the impeller to the bottom of the mini vessel along the vessel centerline.

2.1.2 Agitation System

The mini impeller was attached to a centrally located shaft (diameter 29mm) inside the vessel, rotated by a dissolution system instrument Distek 2100B (Distek Inc., North Brunswick, New Jersey) as shown in Figure 2.4.

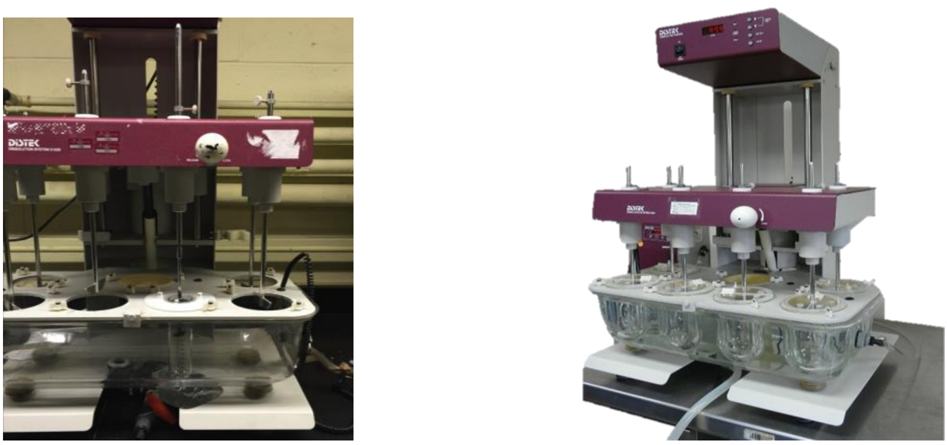

(a) (b)

Figure 2.4 Distek 2100B dissolution apparatus.

2.2 Materials

Three types of spherical particles having average of diameters, d_p, of 11μm, 40μm and 112μm were selected as the disperse phase. The particles were made of silica, (brand name are Sipernat; the advance of these kinds of silica particles are as follow: 1) constant flowability; 2) anti-caking agent; 3) intensive; 4) low dust and were obtained from Evonik (Evonik Industries, Newark, New Jersey). They had the same density, ρ_s, of 2.0 kg/m^3. Tap water at room temperature was used as the liquid medium in all experiments (with density, ρ_L, equal to 977kg/m^3).

2.2.1 Particles Preparatory Procedure

It was noticed, that the suspension contained some fines, which clouded the suspension in preliminary test runs and required a long time (some 10-55minutes) to settle when the agitation was stopped. To remove the fines, the time for the particles of a nominal diameter to settle starting from the air-liquid interface to the vessel bottom (in a 1000mL glass graduated cylinder with round base, Height=430mm) was calculated and found to be 52s for 112μm particles, 5mins for 40μm particles and 55mins for 11μm particles, respectively. The settling times were estimated using Stokes' Law assuming that the particle Reynolds number (Re) during settling was less than one and that the drag coefficient was equal to 24/Re.

Accordingly, when a dense solid particle is placed in a motionless fluid, it will accelerate to a steady-state settling velocity, which is called the free settling velocity. Then the drag force balances the buoyant and gravitational forces of the fluid on the particle. In Newtonian fluids, the free settling velocity (v_t) for spherical particles is a function of different physical and geometrical parameters and it is given by

$$V_t = [\frac{4 g_c d_p (\rho_s - \rho_l)}{3 C_D \rho_l}]^{1/2} \qquad (2.1)$$

In this equation, C_d is the drag coefficient, which directly depends on the particle Reynolds number (Re_p) and particle shape. The expression of the drag coefficient for Stock's Law is defined as $Re_p<1$ and $C_d=24/Re_p$.

During this preparatory procedure, the particles were fully suspended, agitation was stopped, and settling was allowed to take place for only 60s for the 112μm particles and 6mins for the 40μm particles and 60mins for the 11μm particles. At the end of this settling time the supernatant, containing the fines, was removed and it was replaced with fresh tap water. The procedure was repeated three times. No fines were observed in subsequent settling experiments.

2.2.2 Fractions of Solids for Different Operation Conditions

The fractions of solids used in experiments were equal from 0.5% to 0.15% of the liquid weight (w/w), corresponding to about 0.5g for 100mL volume. Table 2.2 gives the amounts and volumes of solids used for each H/T operation conditions.

Table 2.2 Solids Amounts and Volumes Used in Experiments with Different H/T Operation Conditions

H/T	**Solid Amount in Each System (g)**			**Particle Volume Percentage**		
	11 μm	40 μm	112 μm	11 μm	40 μm	112 μm
2.05 (100mL)	0.3	0.3	0.5	0.3	0.3	0.5
3.00 (150mL)	0.4	0.4	0.6	0.27	0.27	0.4
4.01 (200mL)	0.4	0.4	0.6	0.2	0.2	0.3

2.3 Experimental Method and Approach to N_{js} Determination

Before each experiment, the mini vessel was rinsed by tap water. The mini vessel was then filled with tap water to certain volume. The impeller off-bottom clearance, C_b, measured from the bottom of the impeller to the bottom of the mini vessel along the vessel centerline, was set to the required value by moving the whole vessel assembly vertically. The solid particles were then added and a mirror was placed at a 45° angle under the vessel so that the bottom of the mini vessel could be clearly seen. The set up was illuminated with a 100W lamp, as shown in Figure 2.5.

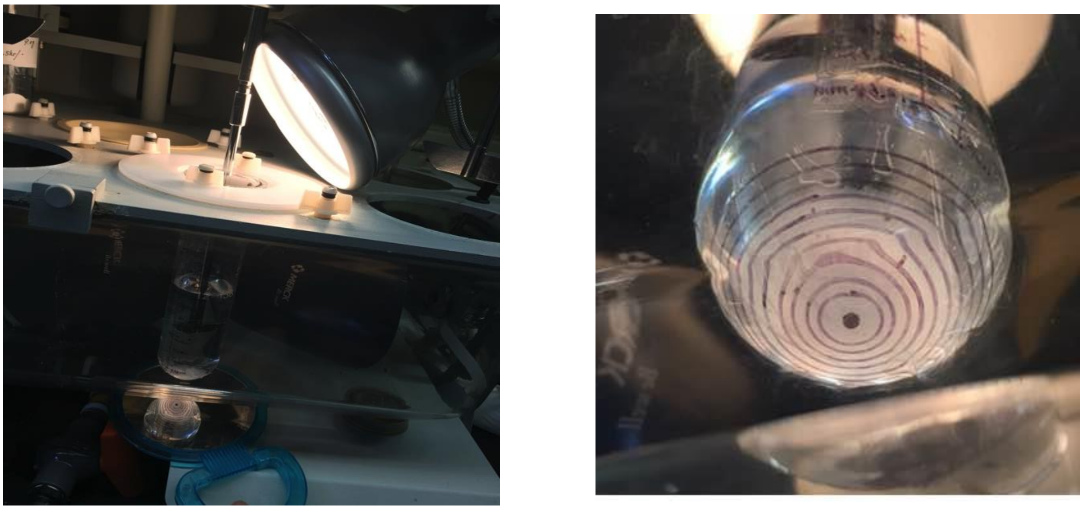

Figure 2.5 A light illuminating from the top of the mini vessel (a) and the image reflected from the mirror.

The approach of the "steady cone radius method" (SCRM) developed by Brucato et al. (2010) was used here to determine N_{js}. These authors studied solid suspension in un-baffled tanks by taking images of the vessel bottom at the different agitation speed at a given value N. They obtained N_{js} by determining the N value at which the inner stationary solids portion would vanish. A typical experiment consisted of setting the agitation speed at a given value N, obtained N_{js} by determining the N value at which the inner stationary solids portion would vanish. Since the vessel bottom had been marked with circles and radii emanating from the vessel bottom center, both the diameter D_s of the area covered by solids at a given N and the corresponding area A_s could be recorded and measured. In this case, the solids covered symmetrically on circular areas, therefore the average values of D_s and A_s were recorded and compared. In a typical experimental set in the hemispherical-bottomed mini vessel system, N values were generally recorded at D_s values equal to 24mm, 22mm, 20mm, 18mm, 16mm, 14mm, 12mm, 10mm, 8mm, 6mm, 4mm. Since the bottom of the mini vessel is a hemispherical shape, diameter of the circles on the curved surface needed be calculated, as shown in Table 2.3.

Then Plots of N vs. D_s and N vs. A_s were then constructed, and linear regression lines were obtained to find the predicted extrapolated values of N when D_s to 0 as well as when A_s to 0.

These values were taken as the expected N_{js} values based on these two approaches, and were labeled respectively as N_{js} - D_s -Method and N_{js} - A_s -Method. Examples of this method are presented in Firgure3. 1. In addition, the visual value of N_{js} (N_{js} -Visual) was obtained using the *Zweitering*'s criterion (Zwietering, 1958), defined as the agitation speed at which no particles were visually observed to be at rest on the vessel bottom for more than one to two seconds. As a result, N_{js} - D_s -Method and N_{js} - A_s -Method were compared to N_{js} (N_{js} -Visual) to determine if this approach is valid.

All experiments were repeated in triplicate. Experiments were conducted in different volumes, using different particle size, as summarized in Table 2.4.

Table 2.3 Calculation of the Diameter of the Circles on the Curved Surface

r (mm) on the curved surface	R (mm) of the bottom	Sin (r/R)	r' (mm) measured by caliper
2	22.36	0.089326	1.99
4	22.36	0.177938	2.97
6	22.36	0.265128	5.93
8	22.36	0.350197	7.83
10	22.36	0.432467	9.67
12	22.36	0.511279	11.43
14	22.36	0.586004	13.10
16	22.36	0.656043	14.67
18	22.36	0.720837	16.12
20	22.36	0.779868	17.44
22	22.36	0.832663	18.62
24	22.36	0.878802	19.65

r: diameter of the curve surface
R: outside diameter of the mini vessel
r': diameter of the circles measured by caliper.

Table 2.4 Summary of Experiment Conditions and Variable Ranges Tested in This Work

Vessel Type	Hemispherical-Bottomed Vessel
Impeller Type	Mini Paddle Impeller
Baffling Condition	Un-baffled (UB)
C_b	10mm, 15mm, 20mm, 25mm, 30mm, 35mm
C_b/T	0.25, 0.375, 0.5, 0.625,0.75, 0.875
Particle Size	11 μm, 40 μm and 112 μm

CHAPTER 3

RESULTS AND DISCUSSION

3.1 Results of Solid Suspension Experiment

3.1.1 Comparison of the N_{js} Values Obtained with the Proposed Methods with Those Obtained with the Conventional *Zwietering's* Approach

Settling of solids is a function of the characteristics of the solids (e.g., type, size, shape, density). When the agitation speed is gradually increased in the vessel filled initially with finely divided solids, some solids will begin to move and even be suspended; as the agitation speed increases, more solids become suspended until all solids are suspended. Further agitation increases will only make the suspension more homogeneous. As mentioned before, there are three states of solid suspension: complete on-bottom solid motion; complete off-bottom solid suspension; uniform solid suspension. Reverse to the partial suspension that all particles are moving on the bottom of the vessel, but they are not all fully suspended, lighter or smaller particle may be fully suspended all the time. The off-bottom solid suspension presents no particle remains on the vessel bottom. All solids move vertically and "uniformity". This state is significant because when such a condition is attained the "coning" phenomena could be removed, as shown in Figure 3.1**.**

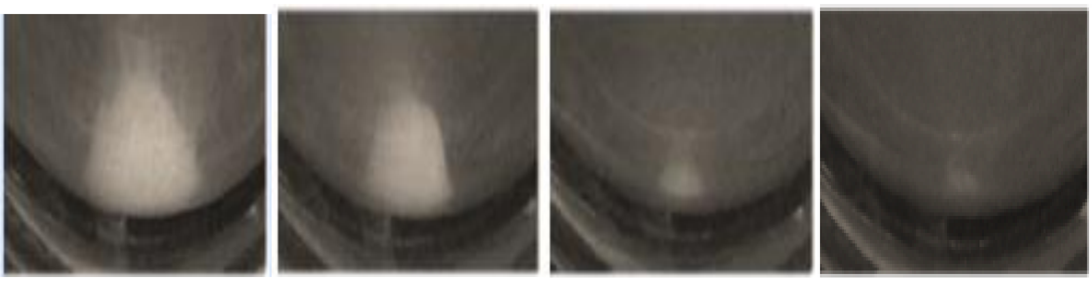

Figure 3.1 Coning eliminating.

In this section, the results of the experiments aimed at validating the N_{js}-D_s -Method and N_{js} - A_s –Method are presented and compared with results obtained by *Zwietering*'s approach, which the N_{js} is defined as the agitation speed at which no particles are visually observed to be at rest on the vessel bottom for more than 1-2 seconds. All experiments were conducted in triplicate.

Figures 3.1-3.3 show a partial results of *N-vs.-*D_s-Method and *N-vs.-*A_s-Method plots for specific operation conditions and the resulting N_{js} values. Appendix A contains a numbered summary of the result for different operation conditions. The values of N_{js} were firstly experimentally obtained in mini paddle equipped with different particle size and operation conditions. It is possible to regress the lines and predict the value of N_{js} at the intersection of each line with the y-axis that since the observation from this figure is that the experimental points align themselves on straight lines (R^2>=0.98), thus identifying the values of N_{js} -A_s-Method and N_{js} -D_s-Method. Regressions of N vs. D_s results in N_{js} values ($N_{js\text{-}Ds}$) that agree very well with the visual N_{js} values ($N_{js\text{-}visual}$). However, the different of N vs. A_s results in N_{js} values ($N_{js\text{-}As}$) is significant. In other words, at least for the mini vessel system, the D_s method is a valid alternative to the conventional method to determine N_{js}.

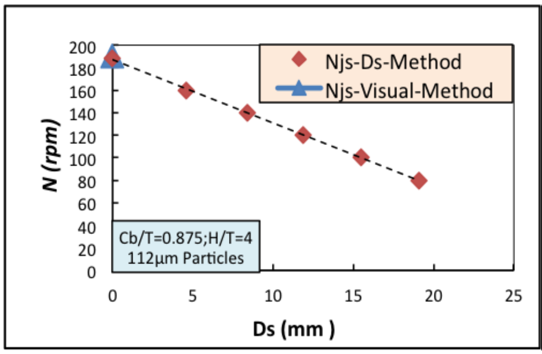

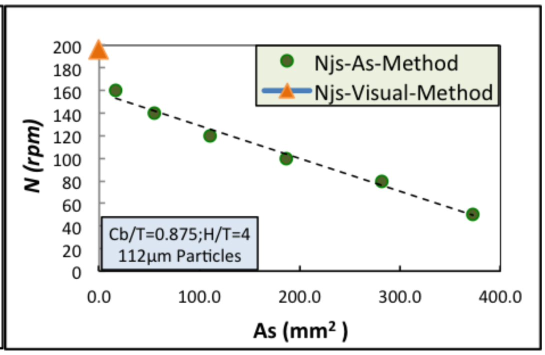

(a) (b)

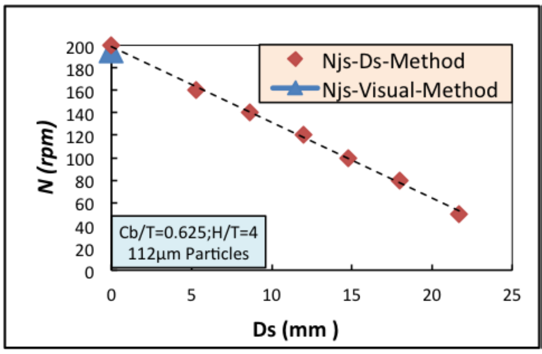

(c)

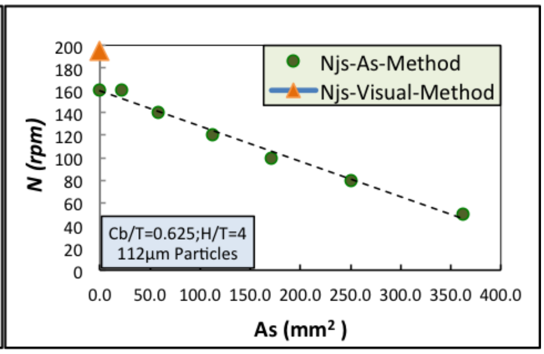

(d)

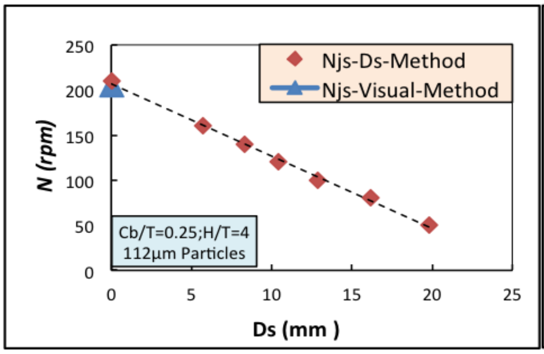

(e)

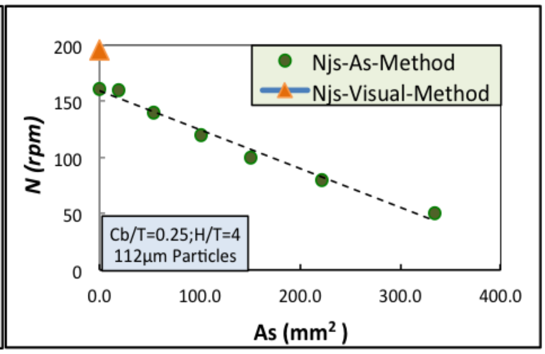

(f)

Figure 3.2 N_{js} obtained in the mini vessel for 112µm particles for H/T=4: (a) N_{js}-D_s Method with C_b=35mm (b) N_{js}-A_s Method with C_b=35mm (c) N_{js}-D_s Method with C_b=25mm (d) N_{js}-A_s Method with C_b=25mm (e) N_{js}-D_s Method with C_b=10mm (f) N_{js}-A_s Method with C_b=10mm.

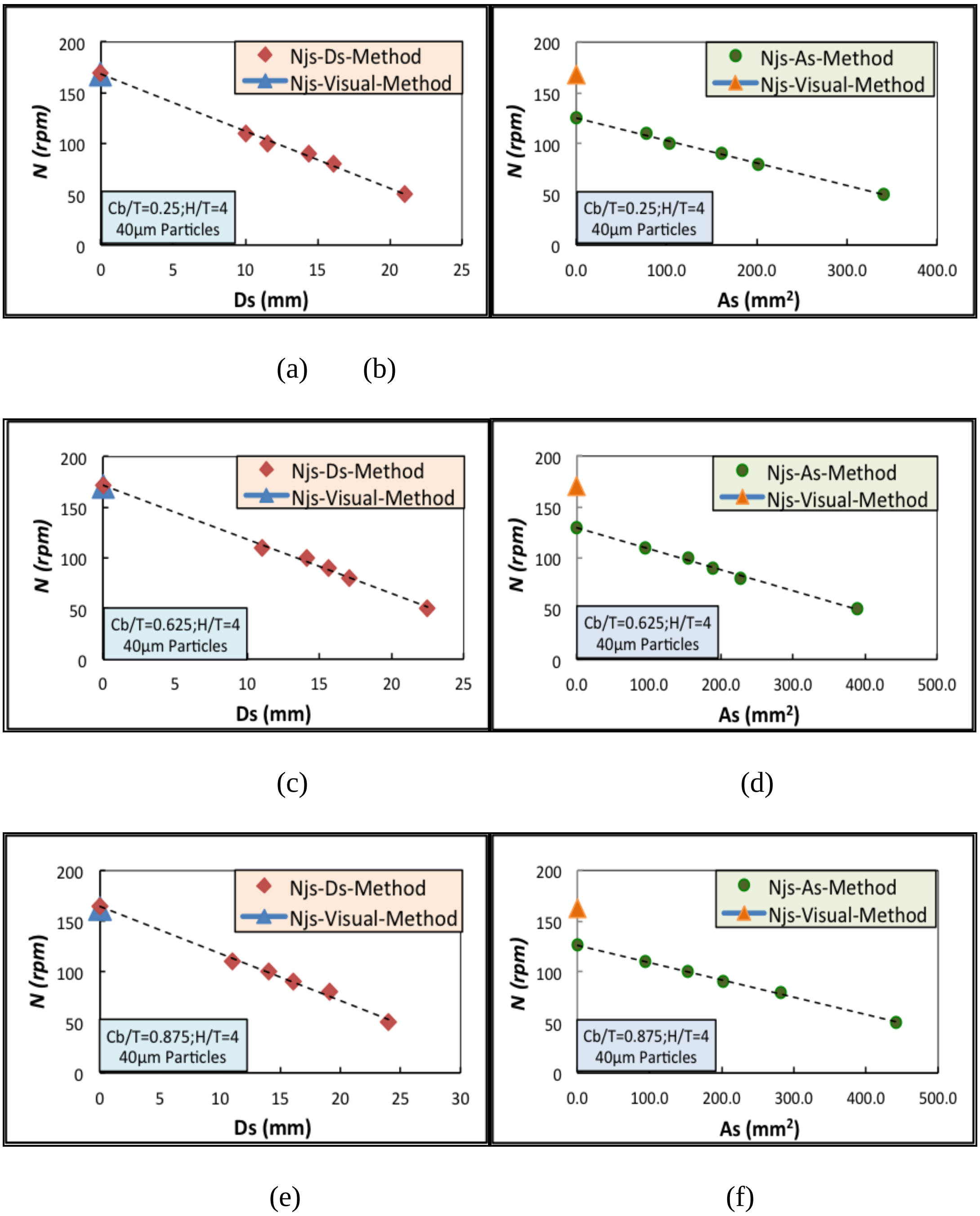

Figure 3.3 N_{js} obtained in the mini vessel for 40µm particles for H/T=4: (a) N_{js}-D_s Method with C_b=35mm (b) N_{js}-A_s Method with C_b=35mm (c) N_{js}-D_s Method with C_b=25mm (d) N_{js}-A_s Method with C_b=25mm (e) N_{js}-D_s Method with C_b=10mm (f) N_{js}-A_s Method with $C_{b=}$10mm.

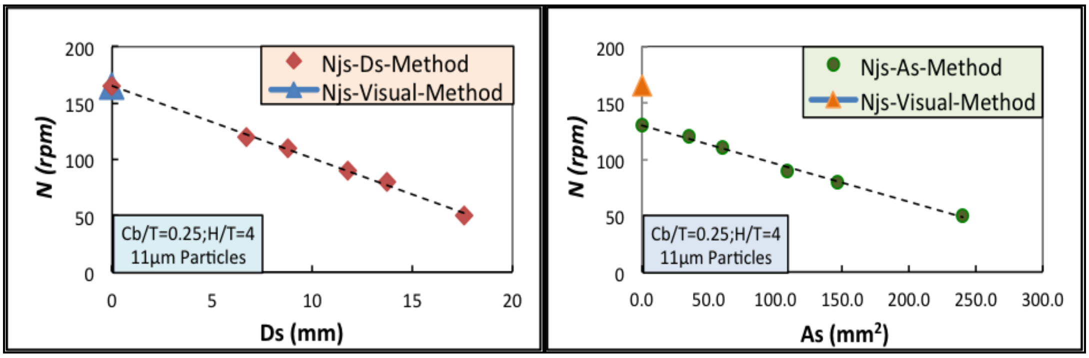

(a) (b)

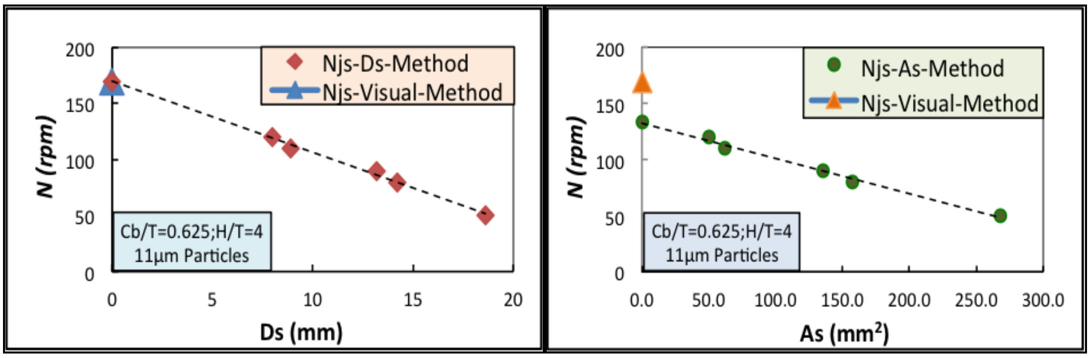

(c) (d)

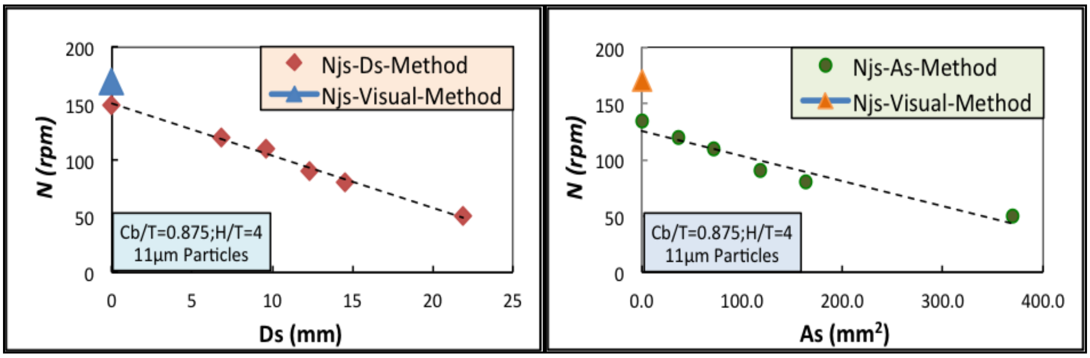

(e) (f)

Figure 3.4 N_{js} obtained in the mini vessel for 11μm particles for H/T=4: (a) N_{js}-D_s Method with C_b=35mm (b) N_{js}-A_s Method with C_b=35mm (c) N_{js}-D_s Method with C_b=25mm (d) N_{js}-A_s Method with C_b=25mm (e) N_{js}-D_s Method with C_b=10mm (f) N_{js}-A_s Method with $C_{b=}$10mm.

3.1.2 Comparison of the Effect of the Mini Paddle Clearance Ratio *Cb/T* on N_{js} under Different Operation Conditions.

Triplicate experiments were conducted with the mini paddle and the standard deviation of triplicate data was calculated for each point. The typical standard deviation was too small (<1%) to be plotted, indicating that the results were highly reproducible. An example of these results is shown in Figure 3.5.

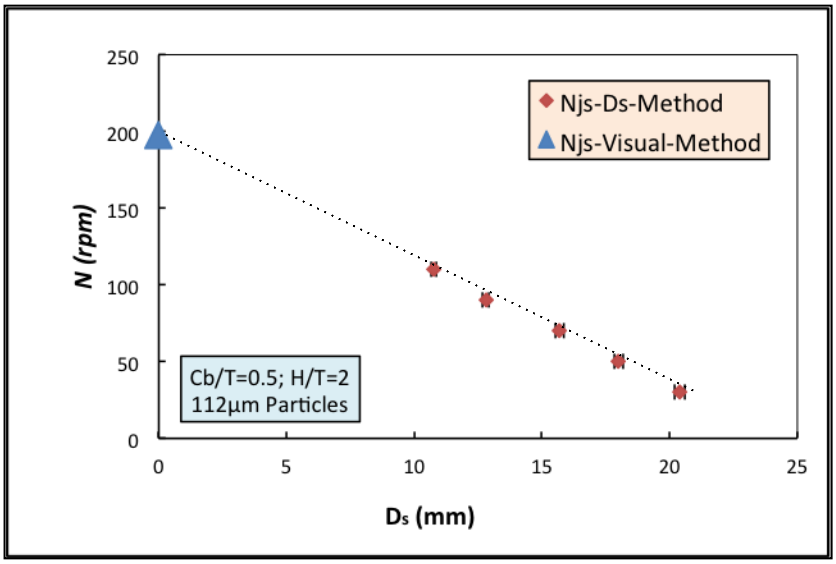

Figure 3.5 Standard Deviation for 112μm particles for H/T=2 with N_{js}-D_s Method.

Increasing the H/T ratio (2<H/T<3) the value of N_{js} increased significantly, but the value of N_{js} increased slightly when continuously increasing the H/T ratio (3<H/T<4). The liquid volume associated with each liquid height, H is shown in Table 3.2, recalling that the internal diameter of the mini vessel (T) is equal to 40.00mm.

Table 3.1 Ratios between H and T

Volume Systems	Ratio (H/T)	Liquid Height (H)
100mL	2.05	82.1mm
150mL	3.00	120.21mm
200mL	4.01	160.38mm

Based on preliminarily validated observed-independent method for determination of N_{js}, results for N_{js} were obtained for variable operation conditions. The results for the mini vessel system with 112μm particles with H/T=2; 3; 4 when the impeller off-bottom ratio (C_b/T) was varied from 0.25 (impeller off-bottom distance=10mm) to 0.875 (impeller off-bottom distance=35mm) are presented in Table 3.2. In addition, results of N_{js} determined with 40μm particles and 11μm particles with H/T=2;3;4 are shown in Table 3.3 and Table 3.4, respectively. Even for these smaller particles, the D_s-method works well to determine N_{js} under the different (C_b/T) operation conditions, while the value of N_{js} in different volume system is very close to each other.

These results show that with different H/T operation conditions, N_{js} can be predicted by N_{js} -Ds-Method. Figure 3.6 shows the variation of N_{js} with H/T=2; 3; 4 operation conditions. N_{js} increases with dp and H/T values.

These results show that N_{js} for the mini paddle is approximatively constant for 0.25<Cb/T<0.75, but that it is slightly lower for Cb/T>0.75 and slightly higher for Cb/T<0.25. The results with the 11μm, 40μm and 112μm particles as dispersed phase are shown in Appendix A.

Table 3.2 Results for N_{js}, 112μm Particles with H/T=4; 3; 2

C_b/T	Particle Size (μm)	Impeller Type	Baffling Type	$N_{js\text{-}Ds\text{-}Method}$ (rpm)	$N_{js\text{-}As\text{-}Method}$ (rpm)	N_{js}-Visual (rpm)
H/T=4						
0.25	112	Mini	UB	206	154	205
0.375	112	Mini	UB	197	160	196
0.5	112	Mini	UB	199	160	198
0.625	112	Mini	UB	199	159	199
0.75	112	Mini	UB	200	161	199
0.875	112	Mini	UB	189	157	189
H/T=3						
0.25	112	Mini	UB	199	160	200
0.375	112	Mini	UB	196	162	196
0.5	112	Mini	UB	198	162	196
0.625	112	Mini	UB	201	163	199
0.75	112	Mini	UB	184	156	183
0.875	112	Mini	UB	180	156	178
H/T=2						
0.25	112	Mini	UB	214	155	215
0.375	112	Mini	UB	198	155	198
0.5	112	Mini	UB	197	137	198
0.625	112	Mini	UB	198	155	198
0.75	112	Mini	UB	195	143	193
0.875	112	Mini	UB	162	124	160

Table 3.3 Results for N_{js}, 40μm Particles with H/T=4; 3; 2

C_b/T	Particle Size (μm)	Impeller Type	Baffling Type	$N_{js\text{-}Ds\text{-}Method}$ (rpm)	$N_{js\text{-}As\text{-}Method}$ (rpm)	$N_{js\text{-}Visual}$ (rpm)
H/T=4						
0.25	40	Mini	UB	170	130	165
0.375	40	Mini	UB	163	131	168
0.5	40	Mini	UB	168	134	166
0.625	40	Mini	UB	172	132	169
0.75	40	Mini	UB	161	133	158
0.875	40	Mini	UB	165	134	149
H/T=3						
0.25	40	Mini	UB	185	137	186
0.375	40	Mini	UB	171	128	170
0.5	40	Mini	UB	172	131	173
0.625	40	Mini	UB	177	136	175
0.75	40	Mini	UB	181	138	179
0.875	40	Mini	UB	148	120	147
H/T=2						
0.25	40	Mini	UB	162	120	162
0.375	40	Mini	UB	142	120	142
0.5	40	Mini	UB	143	116	144
0.625	40	Mini	UB	145	116	145
0.75	40	Mini	UB	147	115	142
0.875	40	Mini	UB	140	113	140

Table 3.4 Results for N_{js}, 11μm Particles with H/T=4; 3; 2

C_b/T	Particle Size (μm)	Impeller Type	Baffling Type	$N_{js\text{-}Ds\text{-}Method}$ (rpm)	$N_{js\text{-}As\text{-}Method}$ (rpm)	N_{js}-Visual (rpm)
H/T=4						
0.25	11	Mini	UB	165	125	168
0.375	11	Mini	UB	167	124	163
0.5	11	Mini	UB	167	126	171
0.625	11	Mini	UB	170	130	171
0.75	11	Mini	UB	161	120	158
0.875	11	Mini	UB	150	126	163
H/T=3						
0.25	11	Mini	UB	158	125	158
0.375	11	Mini	UB	142	113	143
0.5	11	Mini	UB	142	114	142
0.625	11	Mini	UB	144	111	143
0.75	11	Mini	UB	144	114	144
0.875	11	Mini	UB	141	117	141
H/T=2						
0.25	11	Mini	UB	147	119	146
0.375	11	Mini	UB	126	109	125
0.5	11	Mini	UB	128	111	127
0.625	11	Mini	UB	129	112	130
0.75	11	Mini	UB	132	113	131
0.875	11	Mini	UB	131	114	130

In order to better visualize these results, parity plots were generated using the visual values for N_{js} vs. those obtained with the proposed N_{js}-D_s method. The results are presented in Figure 3.7. Panels (a)-(f) show the data for specific systems, whereas Figure 3.8 shows the results for all data systems. In all experiments, one can see that the values of N_{js} -visual agree well with those for N_{js} -Ds-method for different operation conditions. The closer the points align themselves on a 45°-angle-line the better the agreement as shown in Figure 3.8.

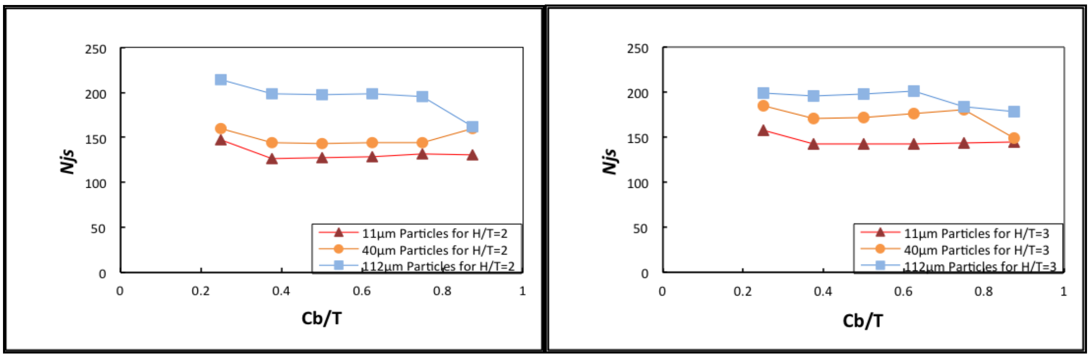

(a) (b)

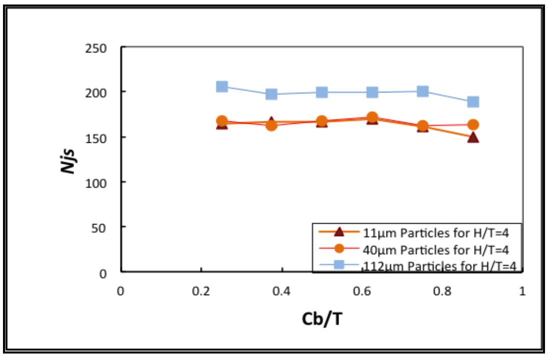

(c)

Figure 3.6 Effect of the mini impeller off-bottom clearance ratio C_b/T on N_{js} for different particles under different H/T operation conditions: (a) H/T=2; (b) H/T=3; (c) H/T=4.

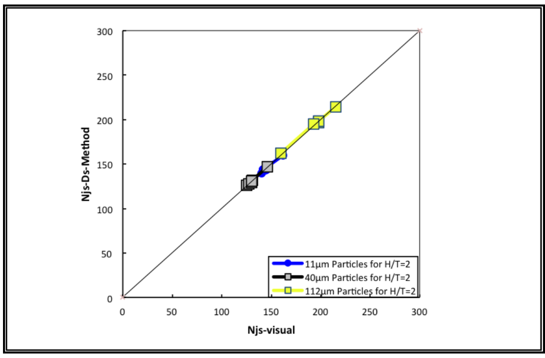

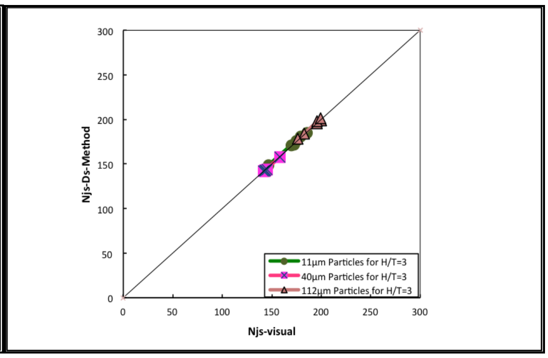

(a) (b)

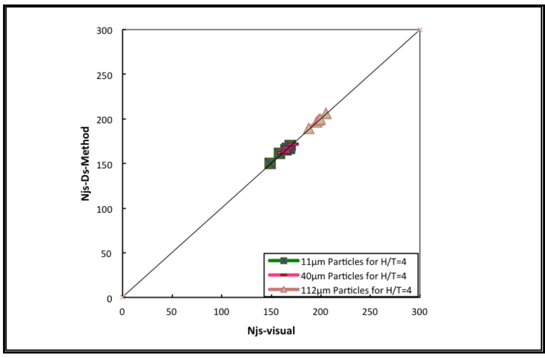

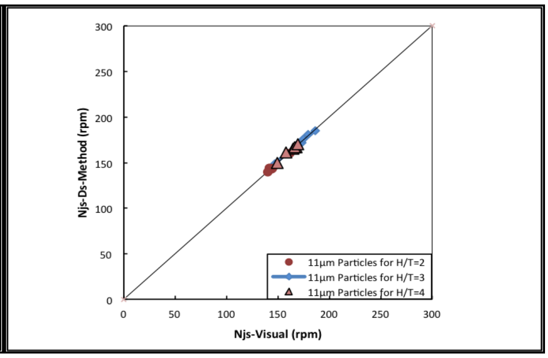

(a) (d)

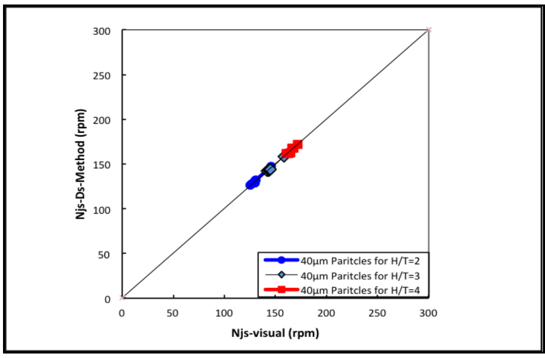

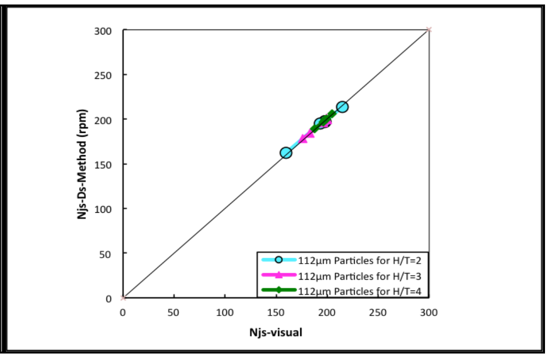

(e) (f)

Figure 3.7 (a) Parity plot for three particle sizes with H/T=2(b) Parity plot for three particle sizes with H/T=3(c) Parity plot for three particle sizes with H/T=4(d) Parity plot for 112μm particle with H/T=2,3,4(e) Parity plot for 40μm particle with H/T=2,3,4(f) Parity plot for 11μm particle with H/T=2,3,4.

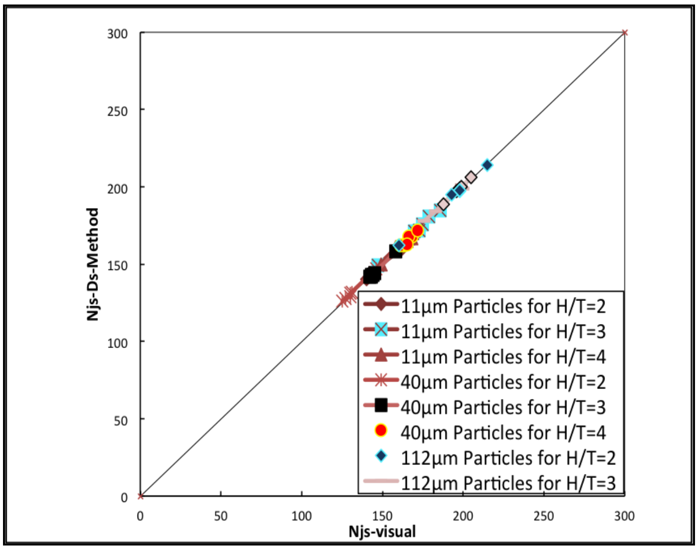

Figure 3.8 Parity plots were generated using the visual values for N_{js} vs. those obtained with the proposed N_{js}-$_{Ds}$ method. The closer the points align themselves on a 45^{o}-angle-line the better the agreement.

3.2 Equations for Minimum Agitation Speed for Solid Suspension, S-Value for Zwietering Equation

Considerable attention has been devoted in the past to the determination of such minimum agitation speed for solid suspension, N_{js}. The pioneering work of Zwietering (1958) still represents the most complete investigation on this subject, in terms of both variety and range of variables studied. His data analysis resulted in an empirical expression for N_{js}:

$$N_{js} = S\frac{v^{0.1} d_p^{0.2}\left(\frac{g\Delta\rho}{\rho_L}\right)^{0.45} X^{0.13}}{D^{0.85}} \qquad (3.1)$$

Base on the Zwietering Equation, the S-values were obtained by fitting the experimental N_{js} data to this equation using as densities 2kg/m^3 (made of silica) and 997.537kg/m^3 for all three particles and for water, respectively. Figure 3.8 shows S-value vs. C_b/T for different system. The s value could be calculated for all the different systems used here by fitting the experimental data for N_{js} to the equations above. Table 3.6-3.8 list this term, which was calculated suing the above relationships and the values of the operating and physical parameters used here. The figure 3.9 shows the *S*-values vs. C_b/T for all different operation conditions. Specific S-value vs. C_b/T operation condition is shown in Appendix B.

Table 3.5 Fitted Zwietering S Values for 112μm Solids

C_b/T	H/T=2	H/T=3	H/T=4
0.25	3.081529056	2.949876756	3.170005762
0.375	2.85113436	2.905406253	3.031510364
0.5	2.836734692	2.935053255	3.062287119
0.625	2.85113436	2.979523759	3.062287119
0.75	2.807935355	2.727524237	3.077675497
0.875	2.332746295	2.638583229	2.908403345

Table 3.6 Fitted Zwietering S Values for 40μm Solids

Cb/T	H/T=2	H/T=3	H/T=4
0.25	2.779340604	3.149005275	3.348309406
0.375	2.382291947	2.830118665	3.228726927
0.5	2.420106105	2.830118665	3.348309406
0.625	2.439013183	2.850049078	3.428031059
0.75	2.49573442	2.850049078	3.228726927
0.875	2.476827341	2.869979491	3.248657341

Table 3.7 Fitted Zwietering S Values for 11μm Solids

Cb/T	H/T=2	H/T=3	H/T=4
0.25	3.916317393	4.773330339	4.257294627
0.375	3.524685654	4.41210534	4.308898198
0.5	3.50020867	4.437907126	4.308898198
0.625	3.524685654	4.541114268	4.386303555
0.75	3.524685654	4.670123196	4.154087484
0.875	3.426777719	3.844466057	3.870267842

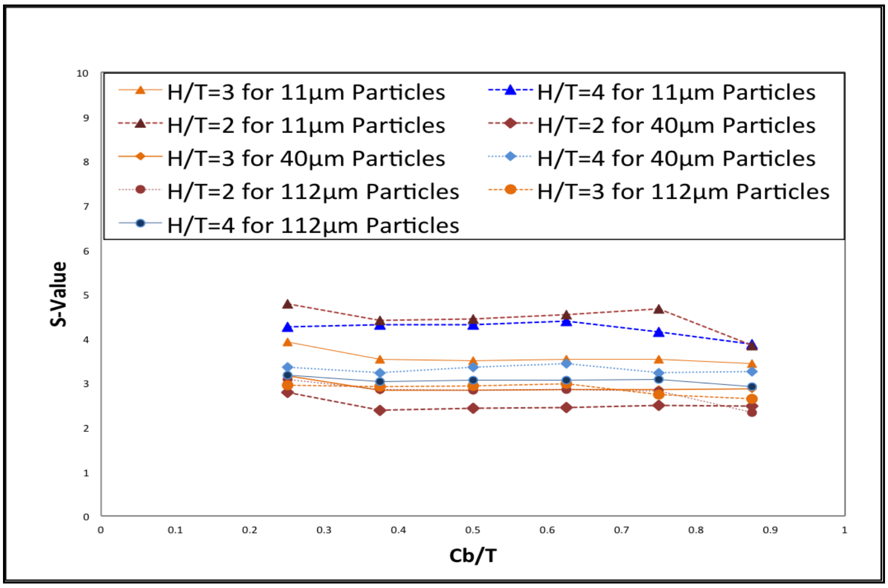

Figure 3.9 *S*-values vs. C_b/T for all different operation conditions.

CHAPTER 4

CONCLUSION

A new method to determine the minimum impeller speed N_{js} (N_{js}-D_s method) to just suspend solids in mini vessel systems (thus removing "coning" effects) was developed here. The results of this method agree well the visually observable values of N_{js} (N_{js} -visual).

N_{js} was experimentally obtained in mini vessels for different operating conditions (*H/T*, d_p and C_b/T) vs. The result could be regressed well with the Zwietering Equation (1958), originally developed for stirred vessels.

The "S" parameter in the Zwietering Equation was obtained for mini vessels, thus enabling the use of this equation to predict when "coning" effects can be eliminated in mini vessel systems during tablet dissolution testing.

In future work, real particle fragments from actual solid dosage products (e.g., prednisone) should be used the test the validity of the results obtained in this study.

APPENDIX A

Figure A.1-A.9 show the N_{js} measured for different particles for all operation conditions.

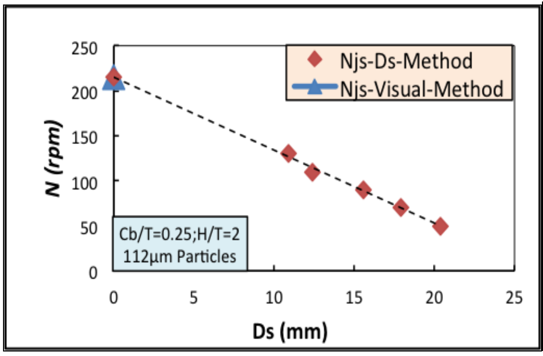

(a)

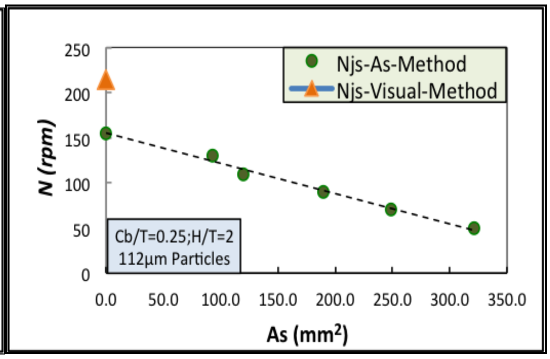

(b)

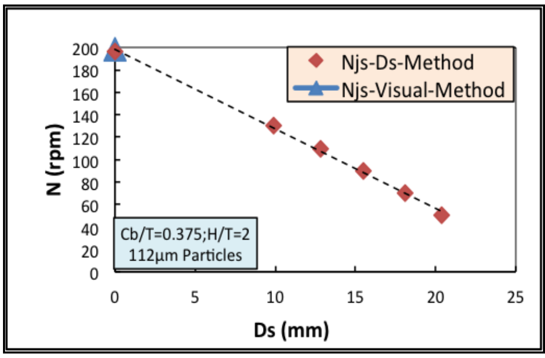

(c)

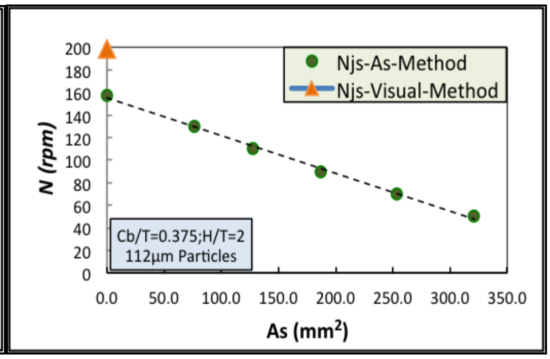

(d)

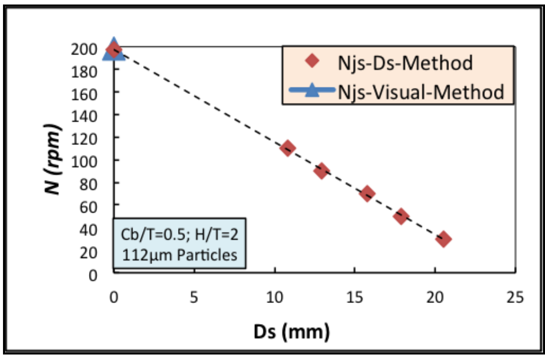

(e)

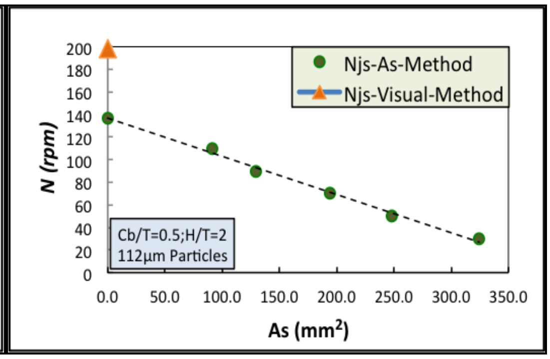

(f)

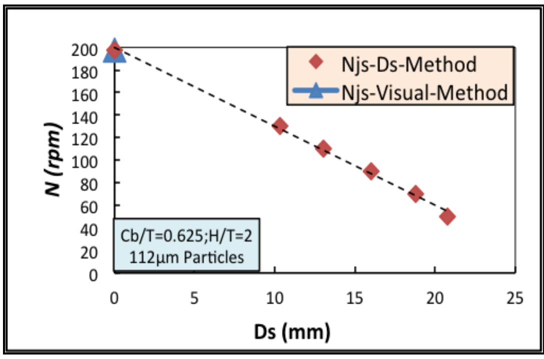

(g)

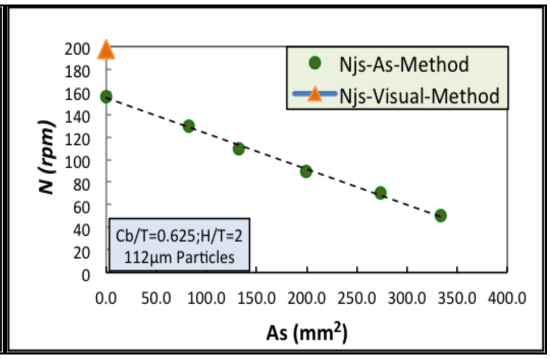

(h)

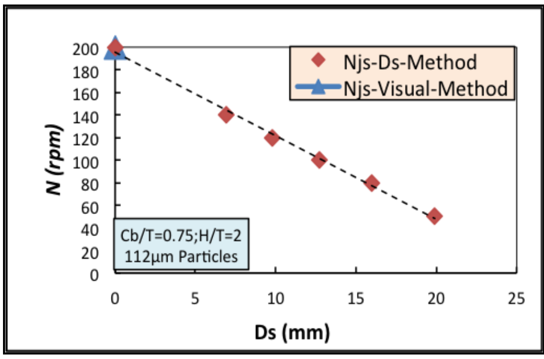

(i)

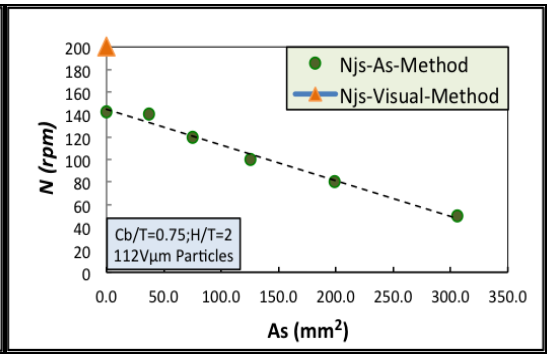

(j)

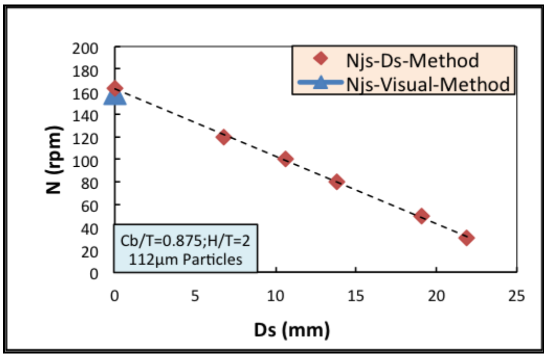

(i)

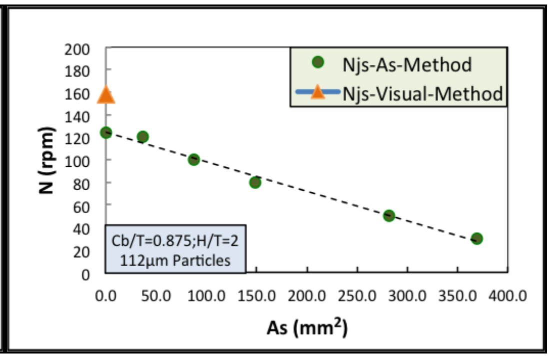

(j)

Figure A.1 N_{js} measured the mini vessel for 112µm particles for H/T=2 with different C_b/T.

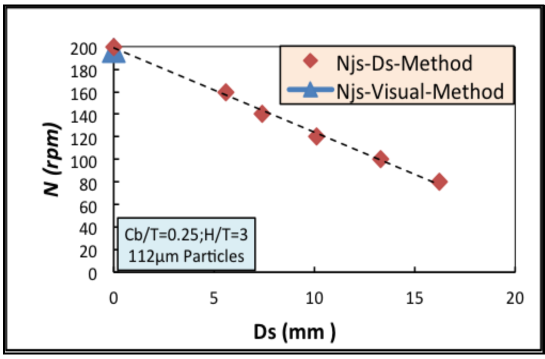
Njs-Ds-Method
Njs-Visual-Method
Cb/T=0.25;H/T=3
112μm Particles
N (rpm)
Ds (mm)

(a)

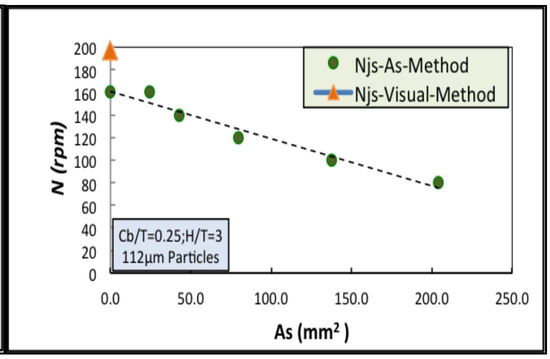
Njs-As-Method
Njs-Visual-Method
Cb/T=0.25;H/T=3
112μm Particles
N (rpm)
As (mm^2)

(b)

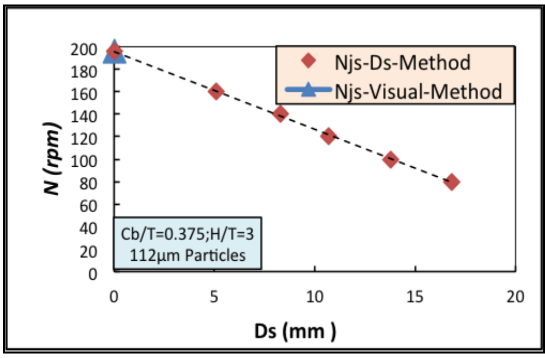
Njs-Ds-Method
Njs-Visual-Method
Cb/T=0.375;H/T=3
112μm Particles
N (rpm)
Ds (mm)

(c)

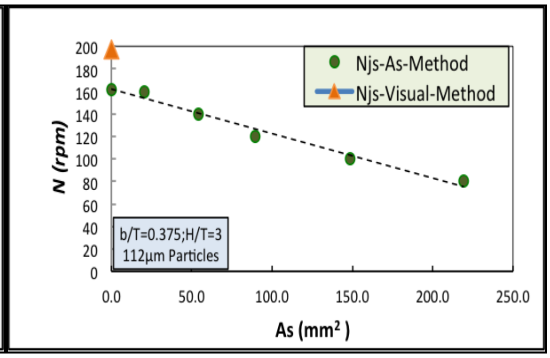
Njs-As-Method
Njs-Visual-Method
b/T=0.375;H/T=3
112μm Particles
N (rpm)
As (mm^2)

(d)

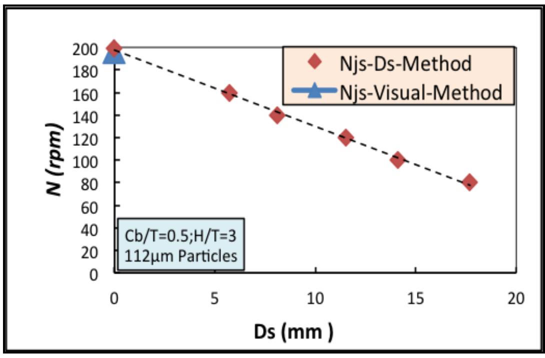
Njs-Ds-Method
Njs-Visual-Method
Cb/T=0.5;H/T=3
112μm Particles
N (rpm)
Ds (mm)

(e)

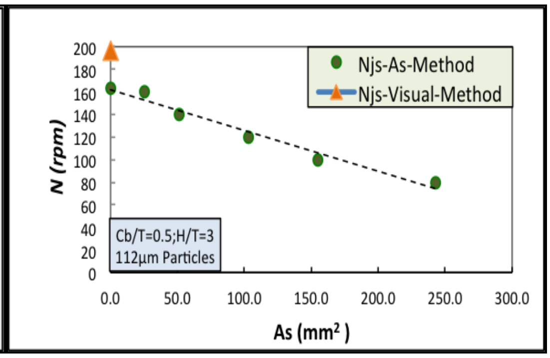
Njs-As-Method
Njs-Visual-Method
Cb/T=0.5;H/T=3
112μm Particles
N (rpm)
As (mm^2)

(f)

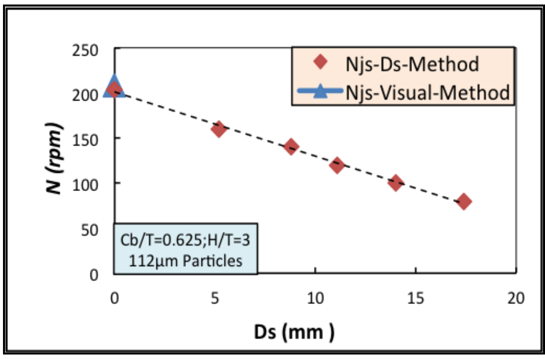

(g)

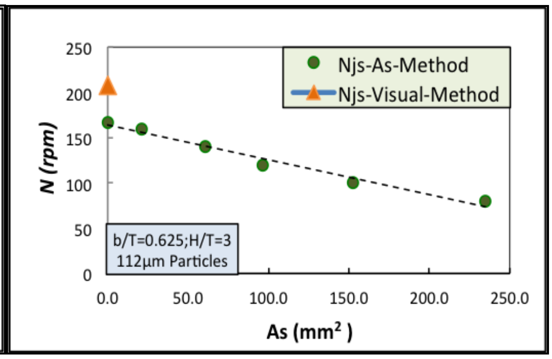

(h)

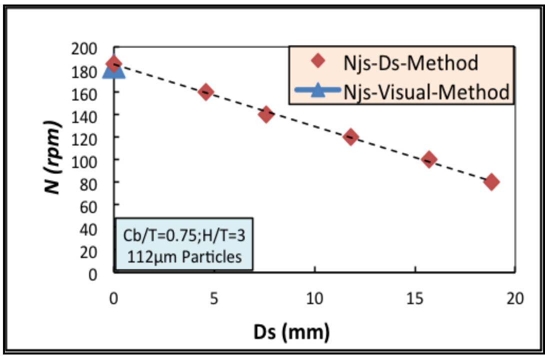

(i)

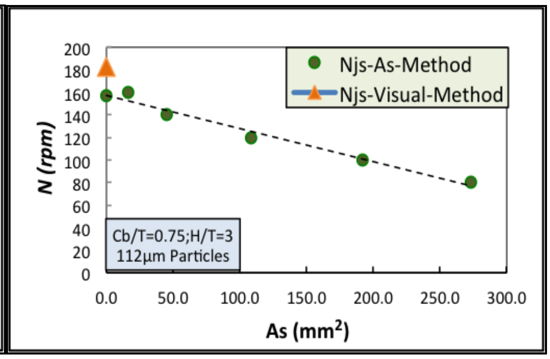

(j)

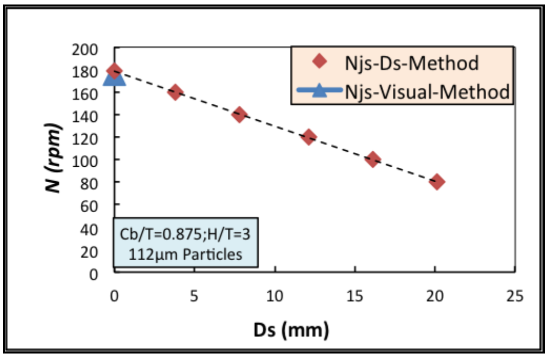

(k)

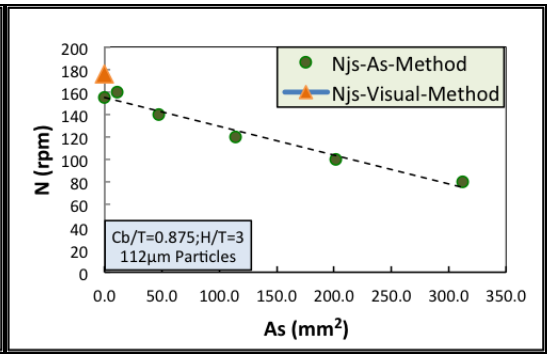

(l)

Figure A.2 N_{js} measured the mini vessel for 112µm particles for H/T=3 with different C_b/T.

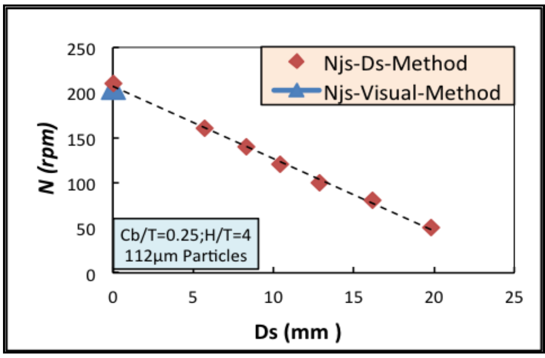
Njs-Ds-Method
Njs-Visual-Method
Cb/T=0.25;H/T=4
112μm Particles
N (rpm)
Ds (mm)
250
200
150
100
50
0
0
5
10
15
20
25

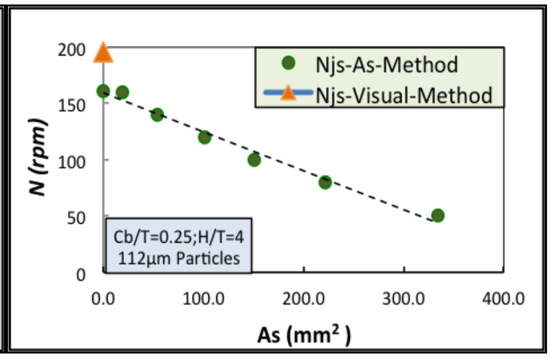
Njs-As-Method
Njs-Visual-Method
Cb/T=0.25;H/T=4
112μm Particles
N (rpm)
As (mm²)
200
150
100
50
0
0.0
100.0
200.0
300.0
400.0

(a) (b)

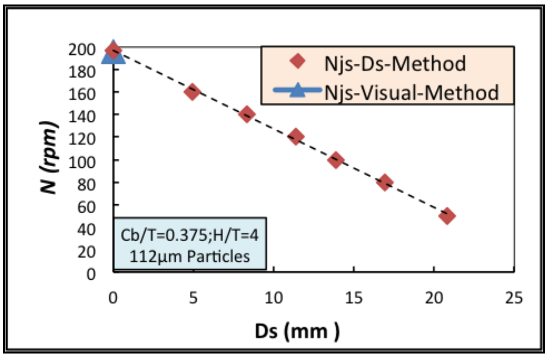
Njs-Ds-Method
Njs-Visual-Method
Cb/T=0.375;H/T=4
112μm Particles
N (rpm)
Ds (mm)
200
180
160
140
120
100
80
60
40
20
0
0
5
10
15
20
25

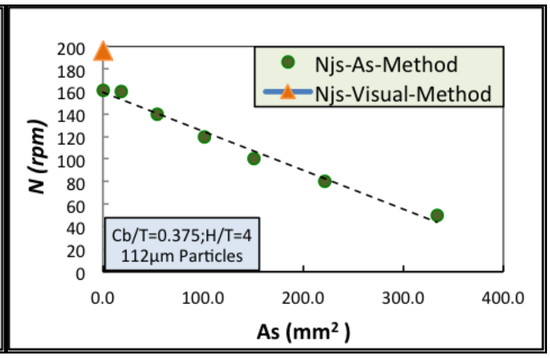
Njs-As-Method
Njs-Visual-Method
Cb/T=0.375;H/T=4
112μm Particles
N (rpm)
As (mm²)
200
180
160
140
120
100
80
60
40
20
0
0.0
100.0
200.0
300.0
400.0

(c) (d)

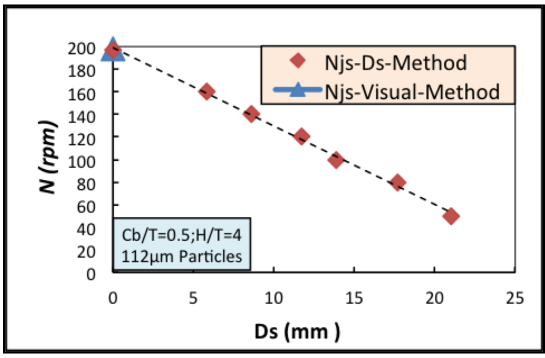
Njs-Ds-Method
Njs-Visual-Method
Cb/T=0.5;H/T=4
112μm Particles
N (rpm)
Ds (mm)
200
180
160
140
120
100
80
60
40
20
0
0
5
10
15
20
25

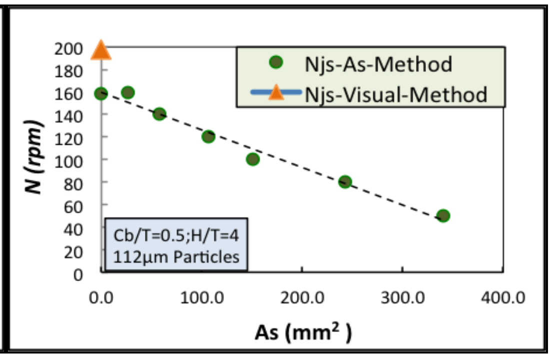
Njs-As-Method
Njs-Visual-Method
Cb/T=0.5;H/T=4
112μm Particles
N (rpm)
As (mm²)
200
180
160
140
120
100
80
60
40
20
0
0.0
100.0
200.0
300.0
400.0

(e) (f)

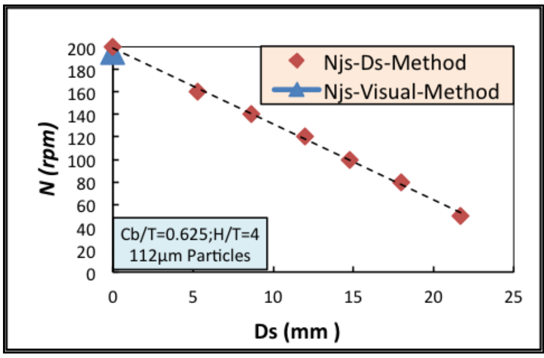

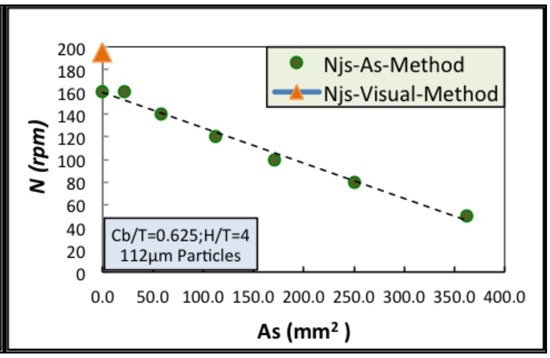

(g) (h)

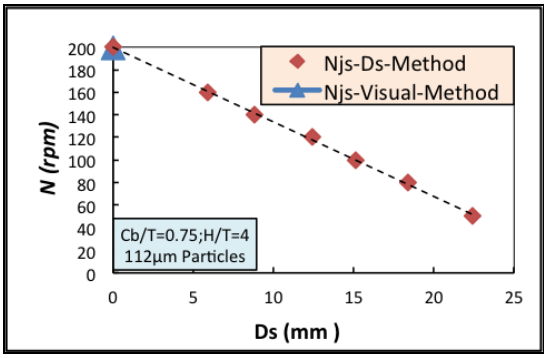

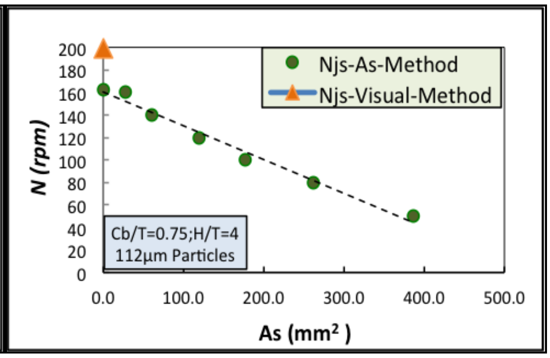

(i) (j)

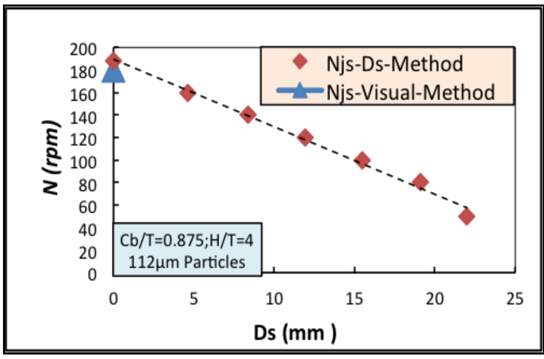

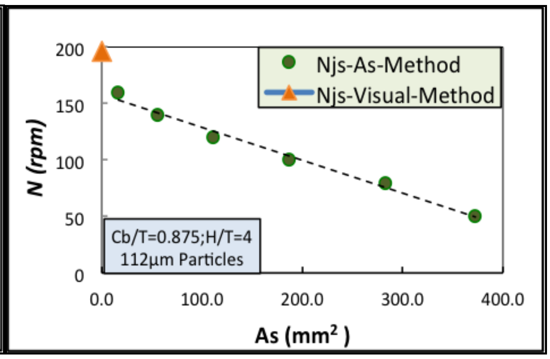

(k) (l)

Figure A.3 N_{js} measured the mini vessel for 112µm particles for H/T=4 with different C_b/T.

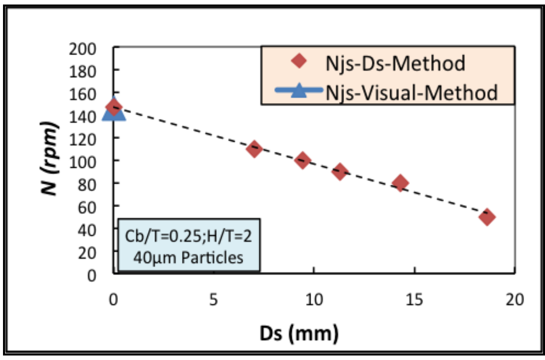
Njs-Ds-Method
Njs-Visual-Method
Cb/T=0.25;H/T=2
40µm Particles
N (rpm)
Ds (mm)

(a)

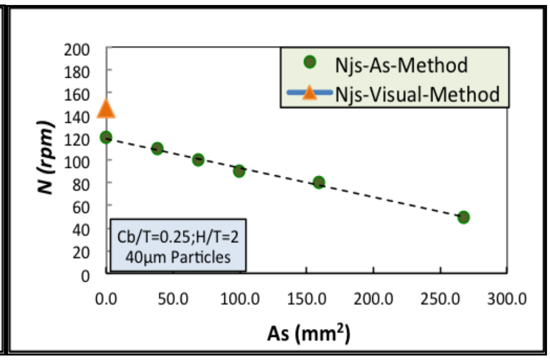
Njs-As-Method
Njs-Visual-Method
Cb/T=0.25;H/T=2
40µm Particles
N (rpm)
As (mm²)

(b)

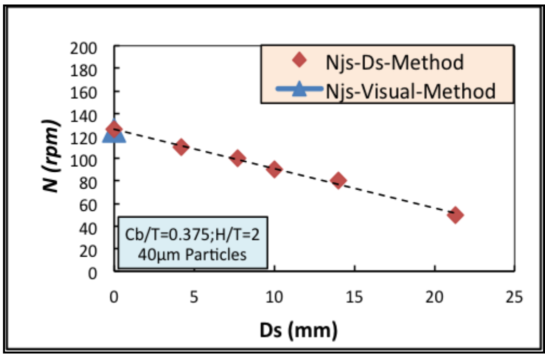
Njs-Ds-Method
Njs-Visual-Method
Cb/T=0.375;H/T=2
40µm Particles
N (rpm)
Ds (mm)

(c)

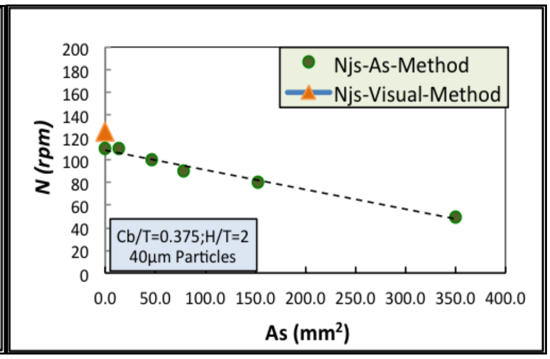
Njs-As-Method
Njs-Visual-Method
Cb/T=0.375;H/T=2
40µm Particles
N (rpm)
As (mm²)

(d)

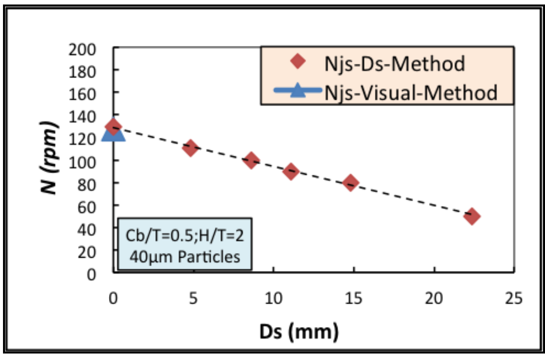
Njs-Ds-Method
Njs-Visual-Method
Cb/T=0.5;H/T=2
40µm Particles
N (rpm)
Ds (mm)

(e)

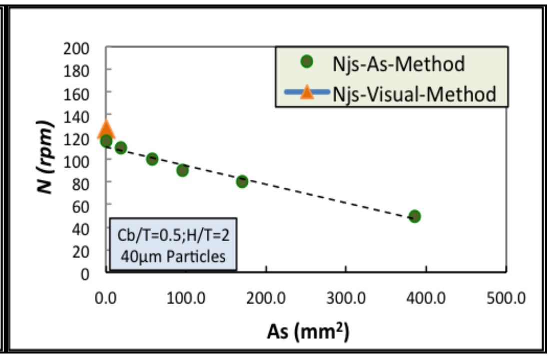
Njs-As-Method
Njs-Visual-Method
Cb/T=0.5;H/T=2
40µm Particles
N (rpm)
As (mm²)

(f)

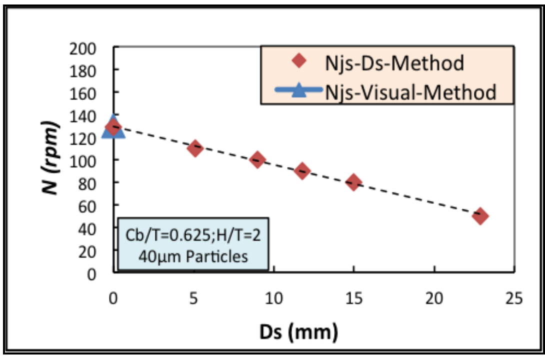

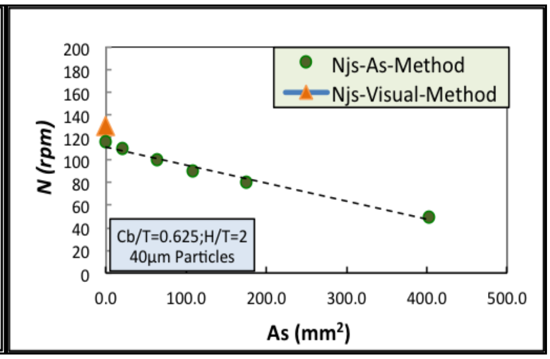

(g) (h)

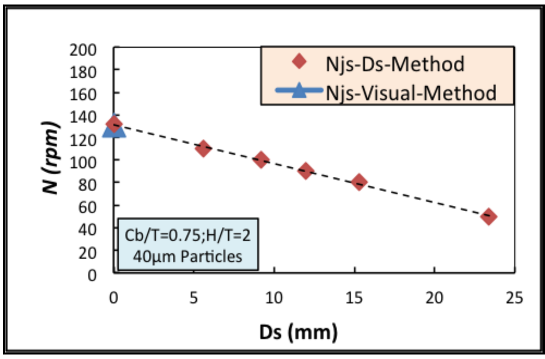

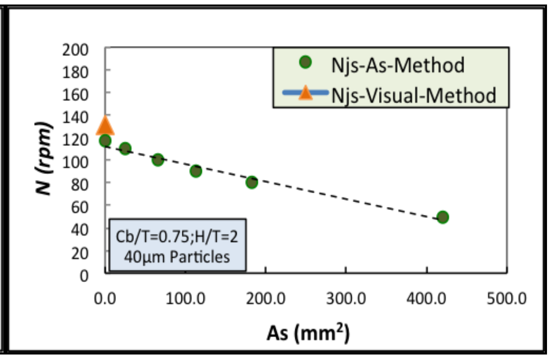

(i) (j)

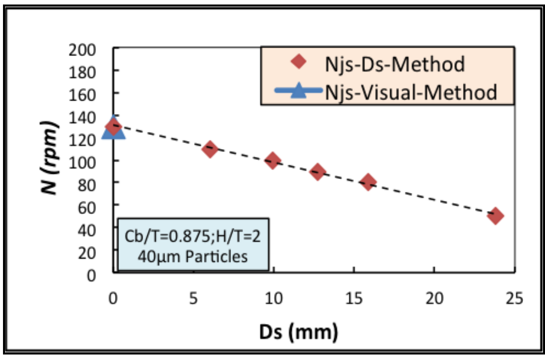

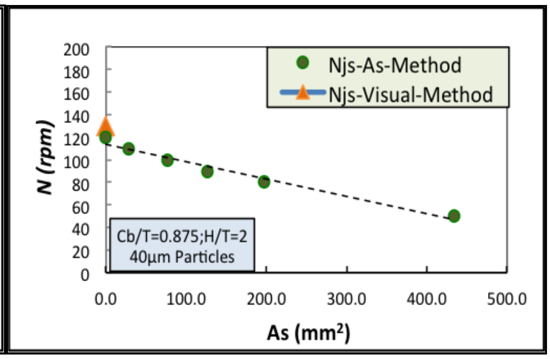

(k) (l)

Figure A.4 N_{js} measured the mini vessel for 40μm particles for H/T=2 with different C_b/T.

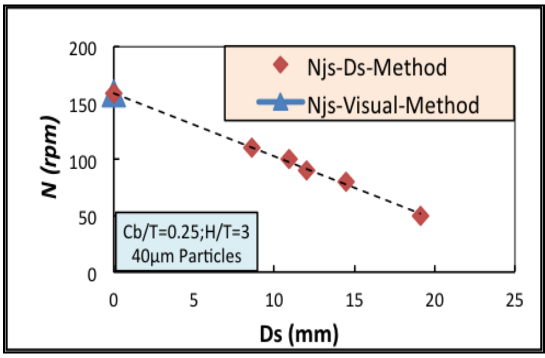
Njs-Ds-Method
Njs-Visual-Method
Cb/T=0.25;H/T=3
40µm Particles
N (rpm)
Ds (mm)
200
150
100
50
0
0
5
10
15
20
25

(a)

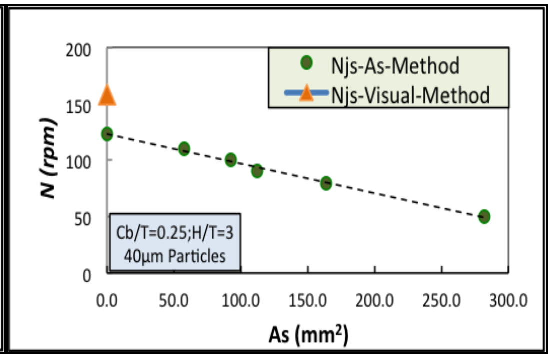
Njs-As-Method
Njs-Visual-Method
Cb/T=0.25;H/T=3
40µm Particles
N (rpm)
As (mm²)
200
150
100
50
0
0.0
50.0
100.0
150.0
200.0
250.0
300.0

(b)

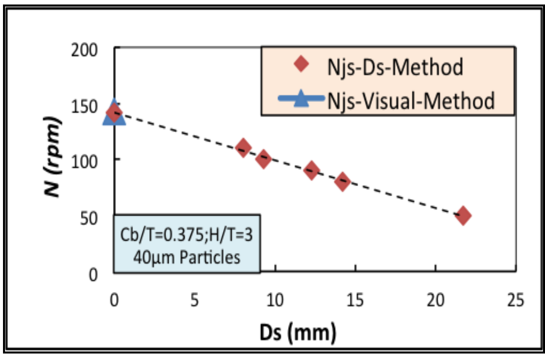
Njs-Ds-Method
Njs-Visual-Method
Cb/T=0.375;H/T=3
40µm Particles
N (rpm)
Ds (mm)
200
150
100
50
0
0
5
10
15
20
25

(c)

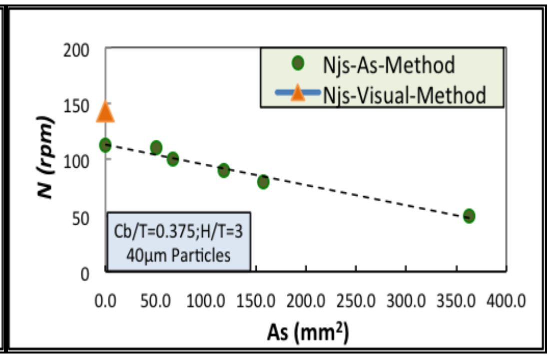
Njs-As-Method
Njs-Visual-Method
Cb/T=0.375;H/T=3
40µm Particles
N (rpm)
As (mm²)
200
150
100
50
0
0.0
50.0
100.0
150.0
200.0
250.0
300.0
350.0
400.0

(d)

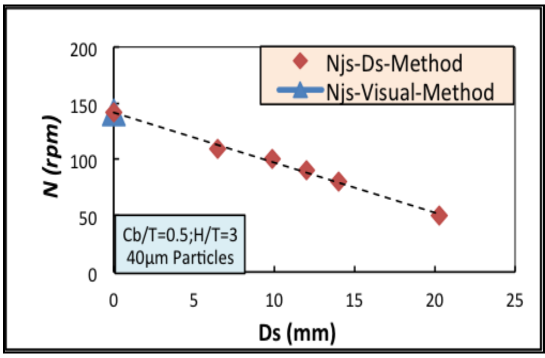
Njs-Ds-Method
Njs-Visual-Method
Cb/T=0.5;H/T=3
40µm Particles
N (rpm)
Ds (mm)
200
150
100
50
0
0
5
10
15
20
25

(e)

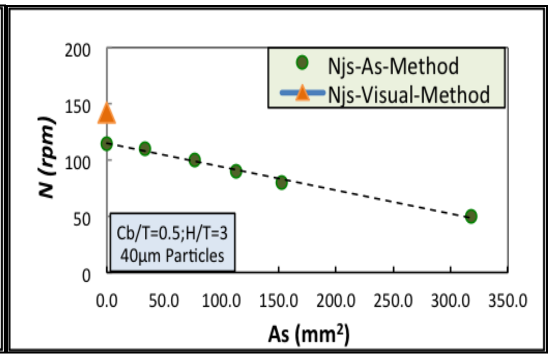
Njs-As-Method
Njs-Visual-Method
Cb/T=0.5;H/T=3
40µm Particles
N (rpm)
As (mm²)
200
150
100
50
0
0.0
50.0
100.0
150.0
200.0
250.0
300.0
350.0

(f)

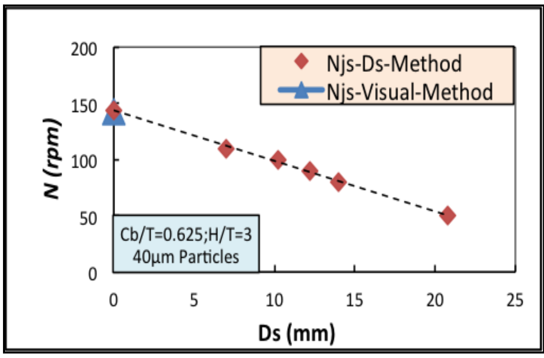

(g)

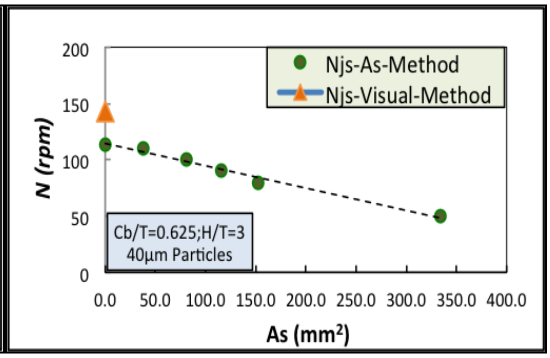

(h)

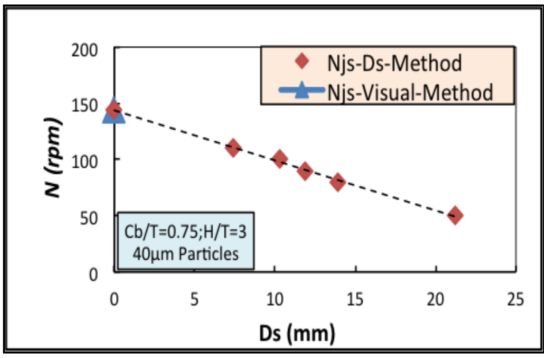

(i)

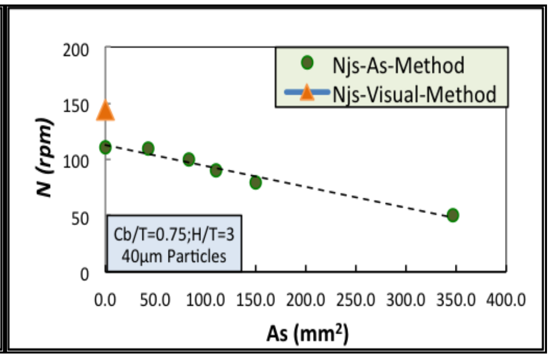

(j)

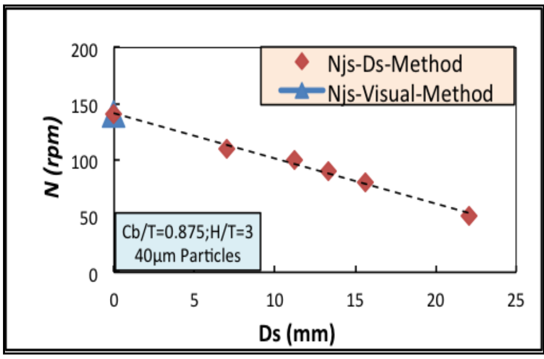

(k)

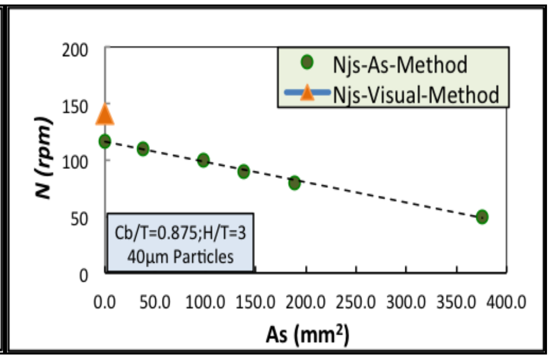

(l)

Figure A.5 N_{js} measured the mini vessel for 40µm particles for H/T=3 with different C_b/T.

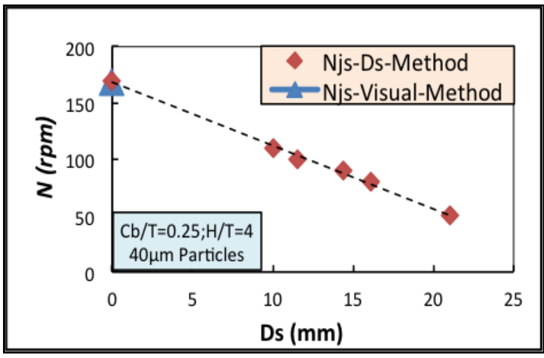
Njs-Ds-Method
Njs-Visual-Method
N (rpm)
200
150
100
50
0
0
5
10
15
20
25
Ds (mm)
Cb/T=0.25;H/T=4
40μm Particles

(a)

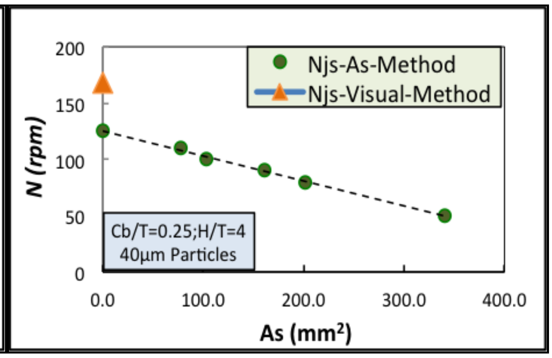
Njs-As-Method
Njs-Visual-Method
N (rpm)
200
150
100
50
0
0.0
100.0
200.0
300.0
400.0
As (mm²)
Cb/T=0.25;H/T=4
40μm Particles

(b)

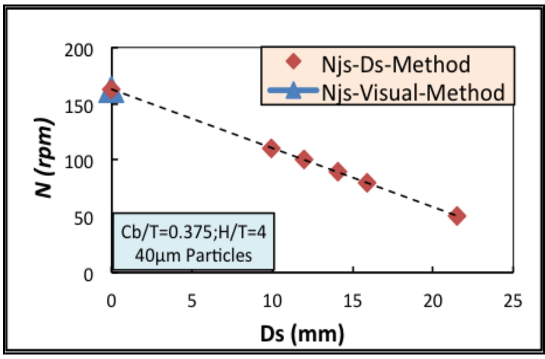
Njs-Ds-Method
Njs-Visual-Method
N (rpm)
200
150
100
50
0
0
5
10
15
20
25
Ds (mm)
Cb/T=0.375;H/T=4
40μm Particles

(c)

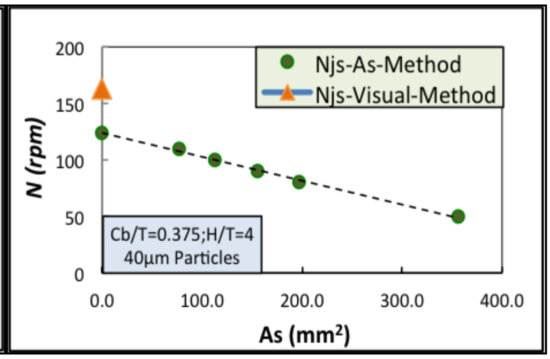
Njs-As-Method
Njs-Visual-Method
N (rpm)
200
150
100
50
0
0.0
100.0
200.0
300.0
400.0
As (mm²)
Cb/T=0.375;H/T=4
40μm Particles

(d)

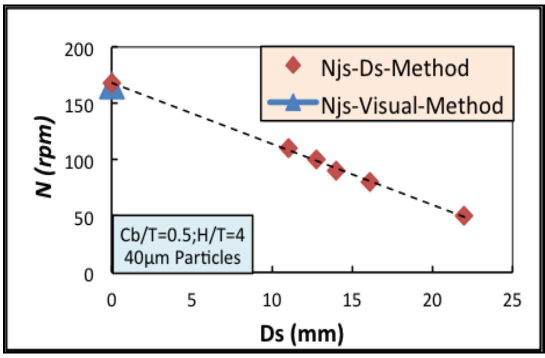
Njs-Ds-Method
Njs-Visual-Method
N (rpm)
200
150
100
50
0
0
5
10
15
20
25
Ds (mm)
Cb/T=0.5;H/T=4
40μm Particles

(e)

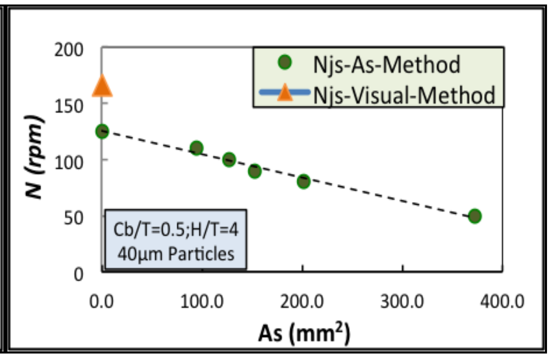
Njs-As-Method
Njs-Visual-Method
N (rpm)
200
150
100
50
0
0.0
100.0
200.0
300.0
400.0
As (mm²)
Cb/T=0.5;H/T=4
40μm Particles

(f)

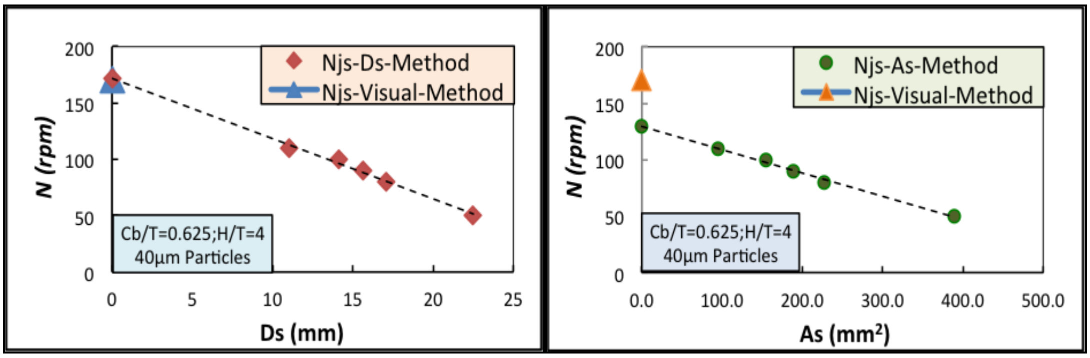

(g) (h)

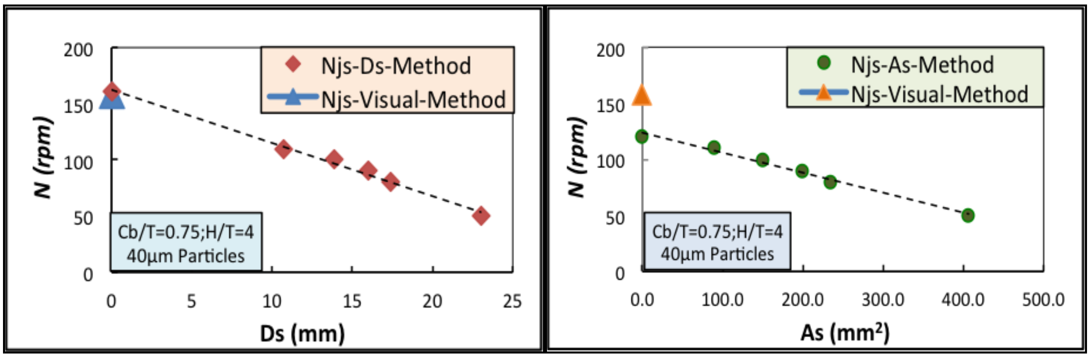

(i) (j)

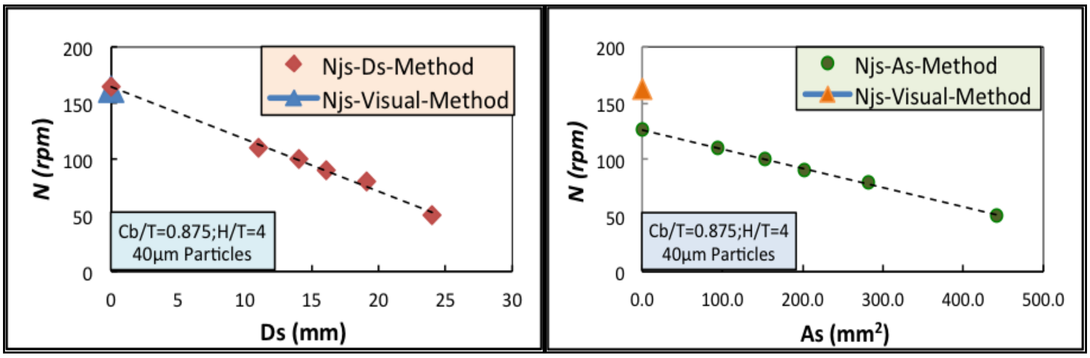

(k) (l)

Figure A.6 N_{js} measured the mini vessel for 40µm particles for H/T=4 with different C_b/T.

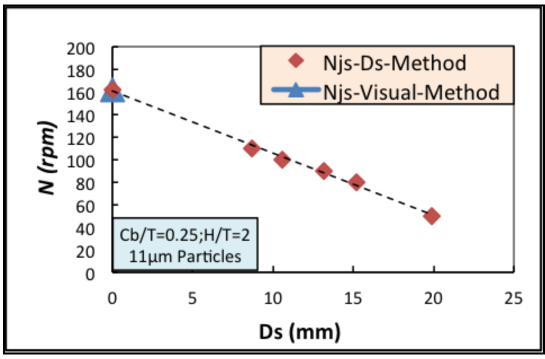
Njs-Ds-Method
Njs-Visual-Method
N (rpm)
Ds (mm)
Cb/T=0.25;H/T=2
11μm Particles
0
20
40
60
80
100
120
140
160
180
200
0
5
10
15
20
25

(a)

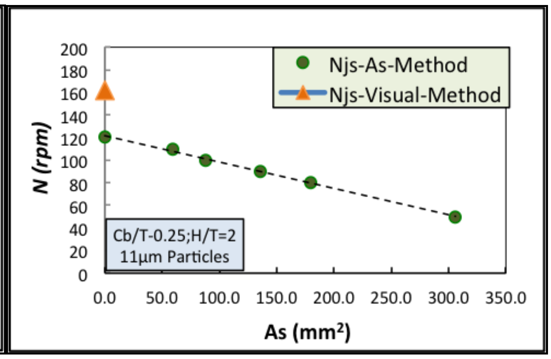
Njs-As-Method
Njs-Visual-Method
N (rpm)
As (mm²)
Cb/T-0.25;H/T=2
11μm Particles
0
20
40
60
80
100
120
140
160
180
200
0.0
50.0
100.0
150.0
200.0
250.0
300.0
350.0

(b)

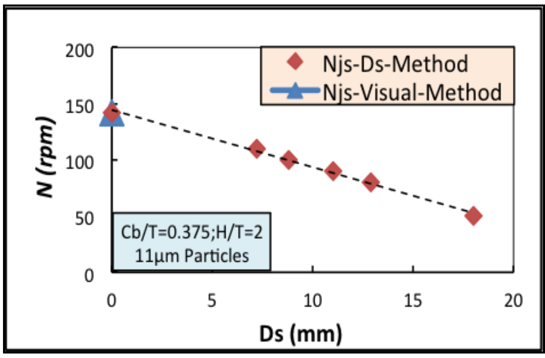
Njs-Ds-Method
Njs-Visual-Method
N (rpm)
Ds (mm)
Cb/T=0.375;H/T=2
11μm Particles
0
50
100
150
200
0
5
10
15
20

(c)

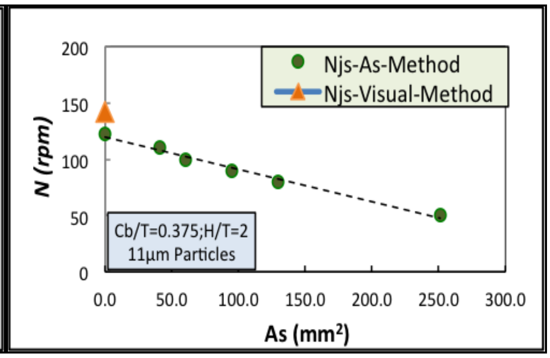
Njs-As-Method
Njs-Visual-Method
N (rpm)
As (mm²)
Cb/T=0.375;H/T=2
11μm Particles
0
50
100
150
200
0.0
50.0
100.0
150.0
200.0
250.0
300.0

(d)

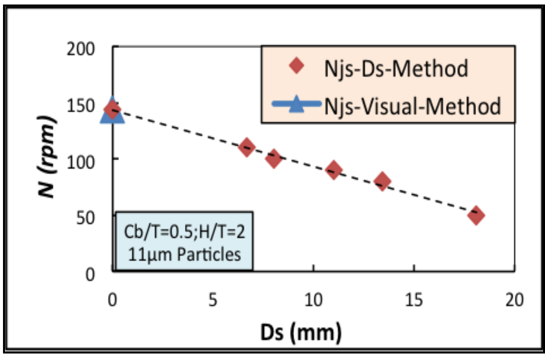
Njs-Ds-Method
Njs-Visual-Method
N (rpm)
Ds (mm)
Cb/T=0.5;H/T=2
11μm Particles
0
50
100
150
200
0
5
10
15
20

(e)

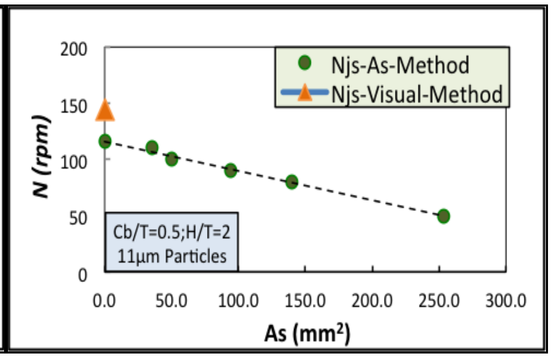
Njs-As-Method
Njs-Visual-Method
N (rpm)
As (mm²)
Cb/T=0.5;H/T=2
11μm Particles
0
50
100
150
200
0.0
50.0
100.0
150.0
200.0
250.0
300.0

(f)

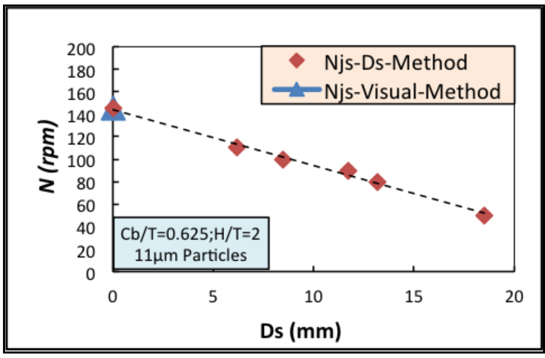

(g)

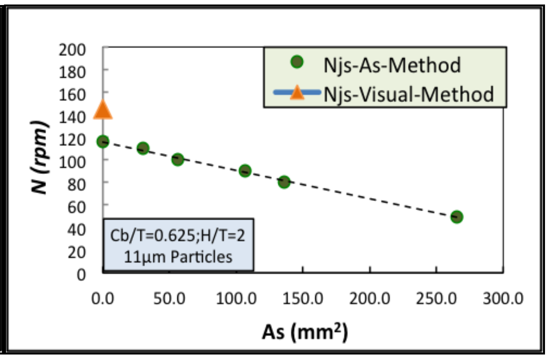

(h)

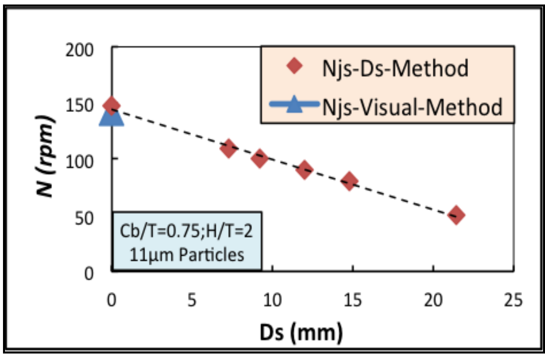

(i)

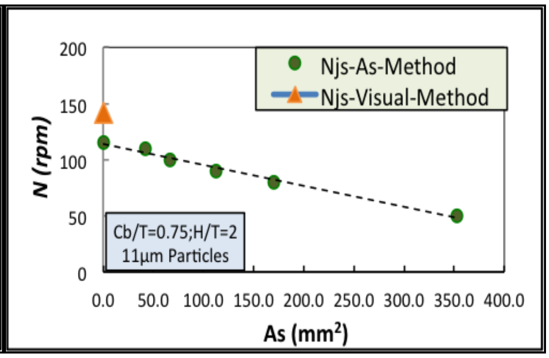

(j)

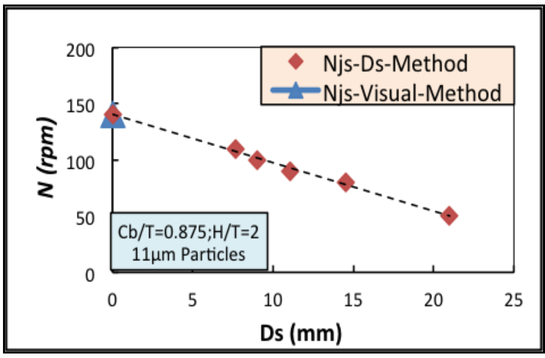

(k)

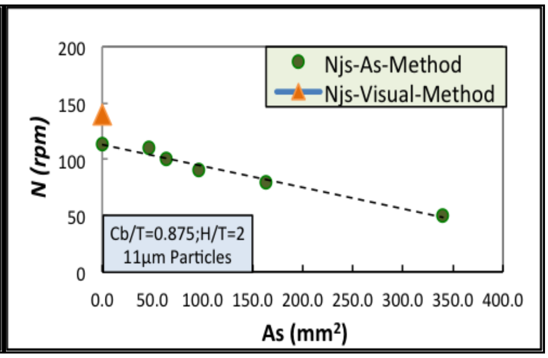

(l)

Figure A.7 N_{js} measured the mini vessel for 11µm particles for H/T=2 with different C_b/T.

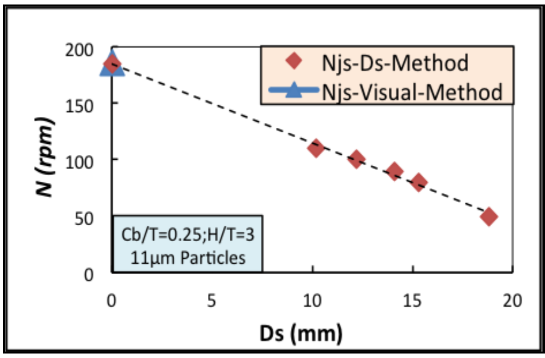
Njs-Ds-Method
Njs-Visual-Method
Cb/T=0.25;H/T=3
11µm Particles
N (rpm)
Ds (mm)
0
50
100
150
200
0
5
10
15
20

(a)

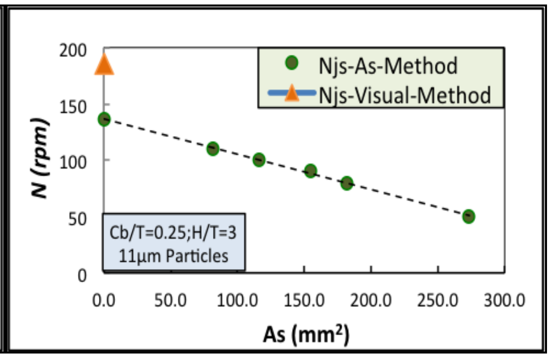
Njs-As-Method
Njs-Visual-Method
Cb/T=0.25;H/T=3
11µm Particles
N (rpm)
As (mm²)
0
50
100
150
200
0.0
50.0
100.0
150.0
200.0
250.0
300.0

(b)

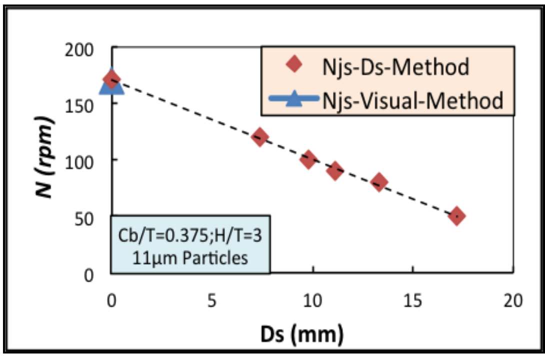
Njs-Ds-Method
Njs-Visual-Method
Cb/T=0.375;H/T=3
11µm Particles
N (rpm)
Ds (mm)
0
50
100
150
200
0
5
10
15
20

(c)

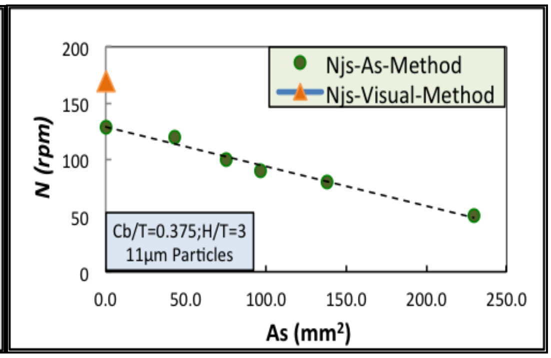
Njs-As-Method
Njs-Visual-Method
Cb/T=0.375;H/T=3
11µm Particles
N (rpm)
As (mm²)
0
50
100
150
200
0.0
50.0
100.0
150.0
200.0
250.0

(d)

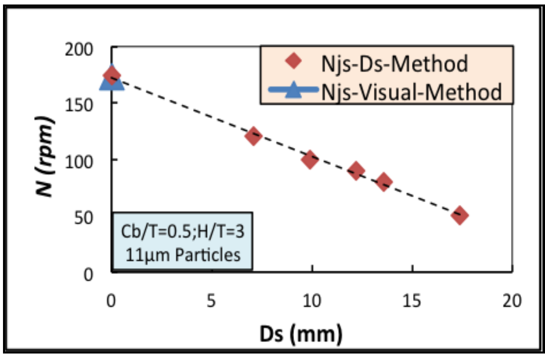
Njs-Ds-Method
Njs-Visual-Method
Cb/T=0.5;H/T=3
11µm Particles
N (rpm)
Ds (mm)
0
50
100
150
200
0
5
10
15
20

(e)

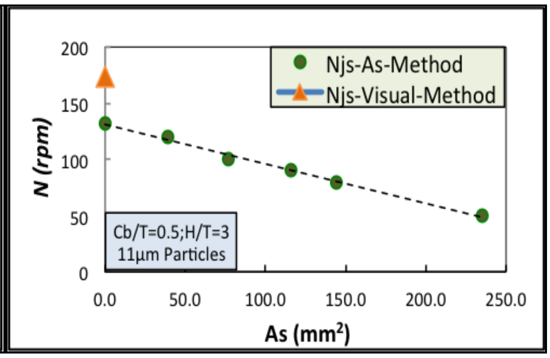
Njs-As-Method
Njs-Visual-Method
Cb/T=0.5;H/T=3
11µm Particles
N (rpm)
As (mm²)
0
50
100
150
200
0.0
50.0
100.0
150.0
200.0
250.0

(f)

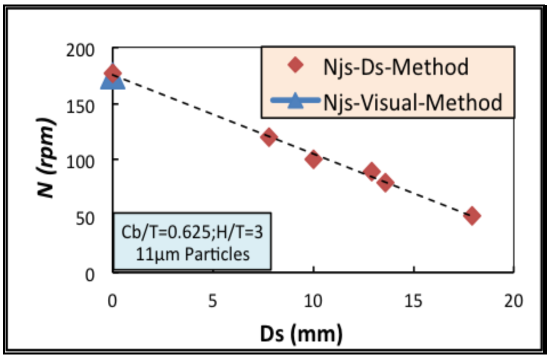

(g)

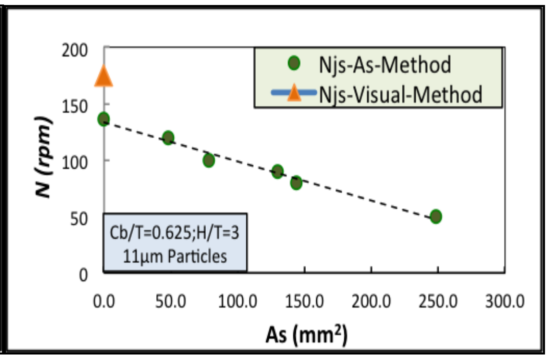

(h)

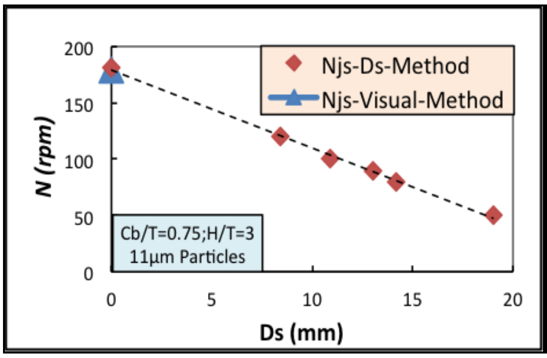

(i)

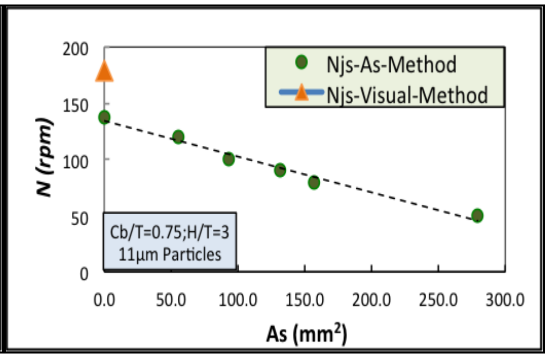

(j)

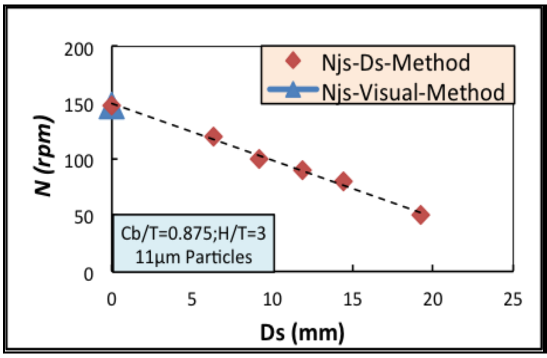

(k)

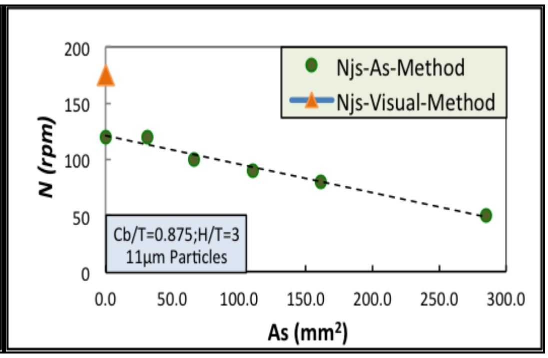

(l)

Figure A.8 N_{js} measured the mini vessel for 11μm particles for H/T=3 with different C_b/T.

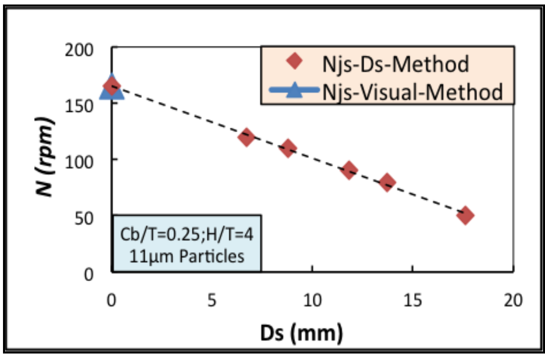
Njs-Ds-Method
Njs-Visual-Method
Cb/T=0.25;H/T=4
11µm Particles
N (rpm)
Ds (mm)
0
50
100
150
200
0
5
10
15
20

(a)

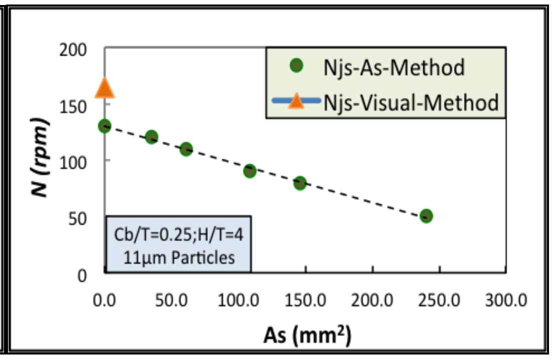
Njs-As-Method
Njs-Visual-Method
Cb/T=0.25;H/T=4
11µm Particles
N (rpm)
As (mm²)
0
50
100
150
200
0.0
50.0
100.0
150.0
200.0
250.0
300.0

(b)

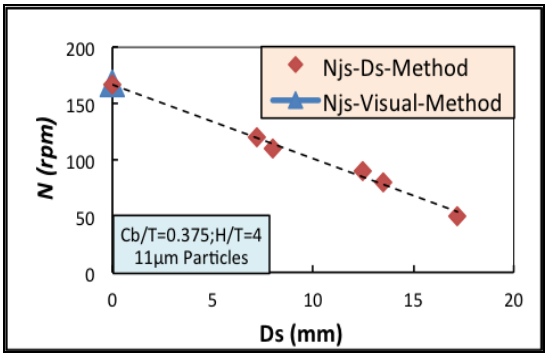
Njs-Ds-Method
Njs-Visual-Method
Cb/T=0.375;H/T=4
11µm Particles
N (rpm)
Ds (mm)
0
50
100
150
200
0
5
10
15
20

(c)

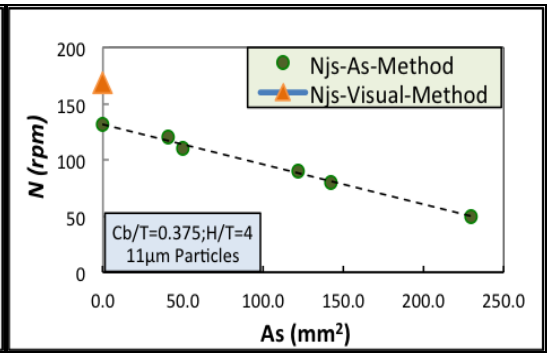
Njs-As-Method
Njs-Visual-Method
Cb/T=0.375;H/T=4
11µm Particles
N (rpm)
As (mm²)
0
50
100
150
200
0.0
50.0
100.0
150.0
200.0
250.0

(d)

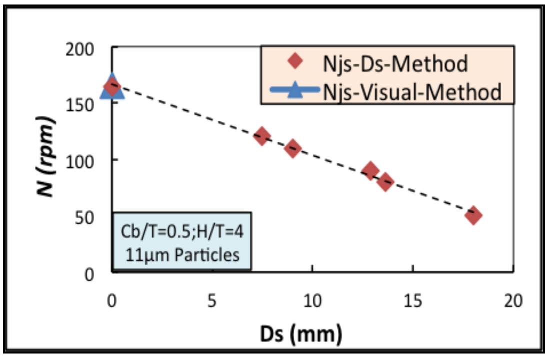
Njs-Ds-Method
Njs-Visual-Method
Cb/T=0.5;H/T=4
11µm Particles
N (rpm)
Ds (mm)
0
50
100
150
200
0
5
10
15
20

(e)

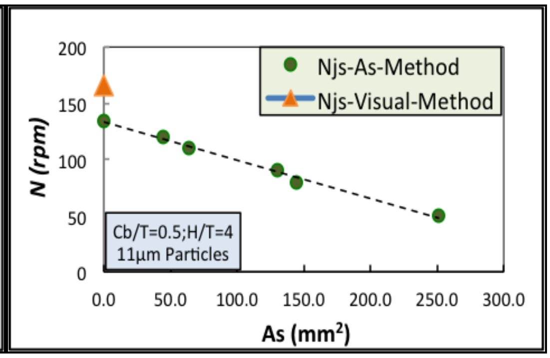
Njs-As-Method
Njs-Visual-Method
Cb/T=0.5;H/T=4
11µm Particles
N (rpm)
As (mm²)
0
50
100
150
200
0.0
50.0
100.0
150.0
200.0
250.0
300.0

(f)

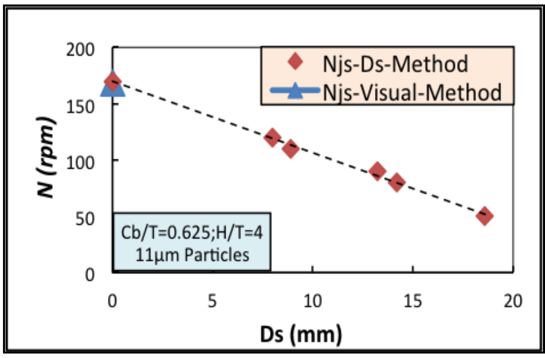

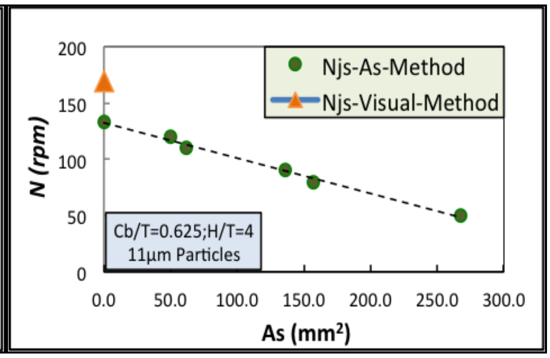

(g) (h)

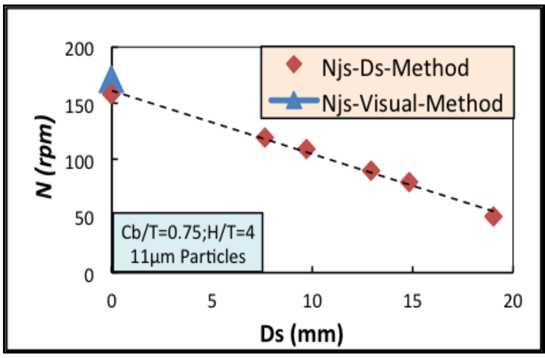

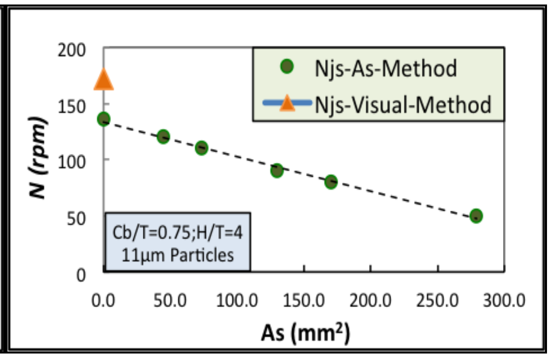

(i) (j)

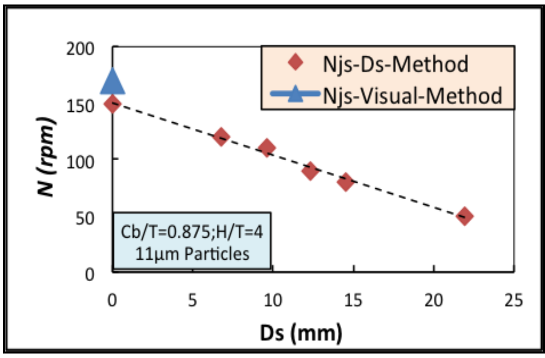

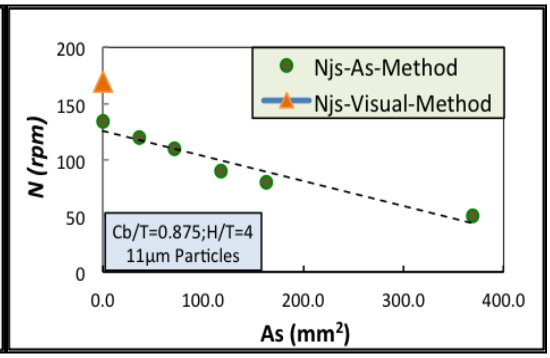

(k) (l)

Figure A.9 N_{js} measured the mini vessel for 11μm particles for H/T=4 with different C_b/T.

APPENDIX B

Figure B.1 shows the S-value for different operation conditions.

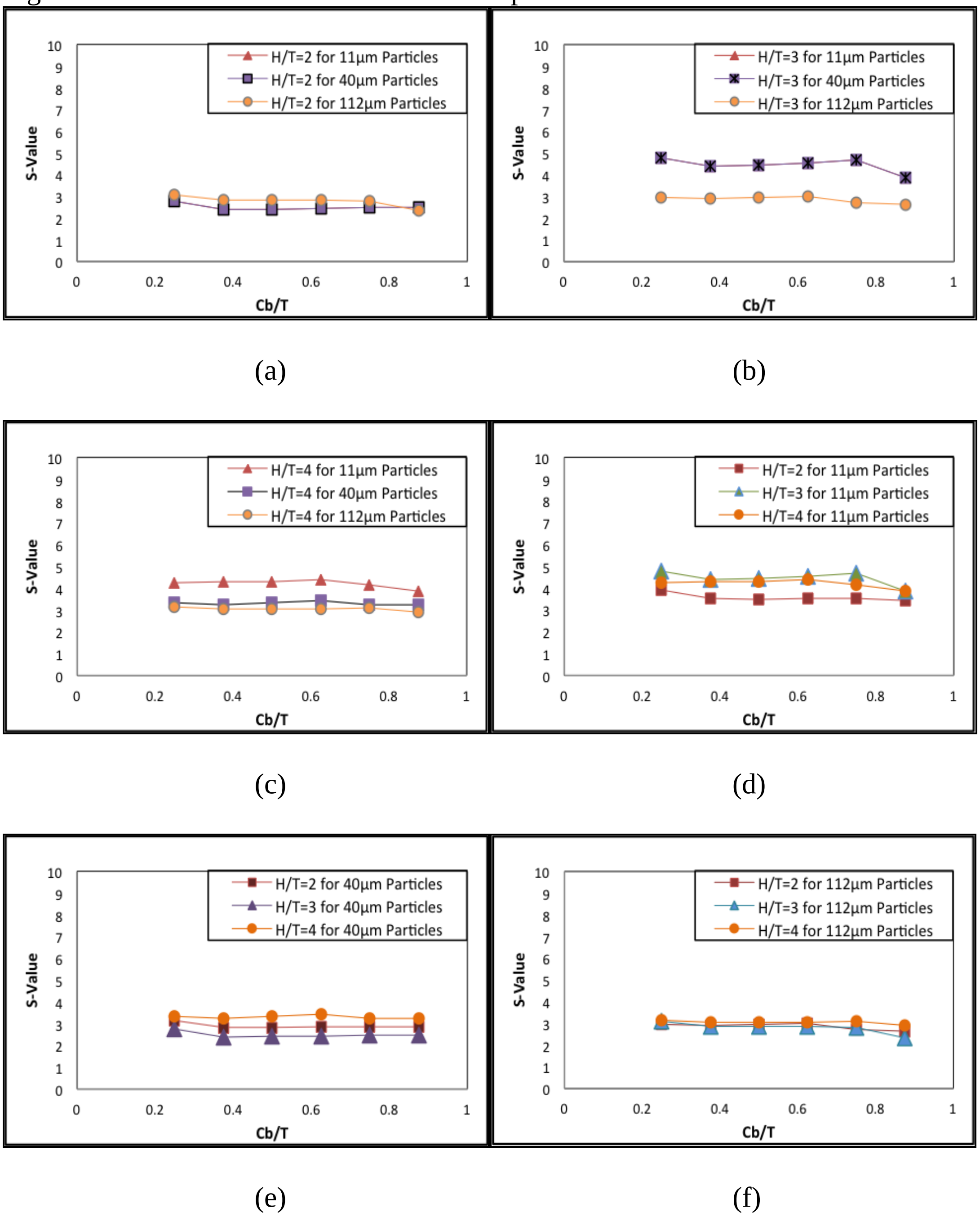

Figure B.1 S value for different operation conditions.

REFERENCES

Armenante, P. M., Uehara-Nagamine, E., Susanto J., "Determination of correlations to predict the minimum agitation speed for complete solid suspension in agitated vessels." *Canadian Journal of Chemical Engineering*, 76, pp. 413-419(1998).

Armenante, P. M., Uehara-Nagamine, E., "Effect of low off- bottom impeller clearance on the minimum agitation speed for complete suspension of solids in stirred tanks." *Chemical Engineering Science*, 53(9), pp. 1757-1775(1998).

Baldi, G., R. Conti and E. Alaria., "Complete Suspension of Particles in Mechanically Agitated Vessels." *Chemical Engineering Science*, 33, pp. 21-25(1978).

Inci A., Marcio B. M., Adam M. M., "Effect of geometry on the mechanisms for off-bottom solids suspension in a stirred tank." *Chemical Engineering Science*, 79, pp. 163-176(2012).

Zwietering, Th. N., "Suspending of solid particles in liquid by agitators." *Chemical Engineering Science*, 8, pp. 244-253(1958).

Sandra K.,Vinod P. S., "A standardized mini paddle apparatus as an alternative to the standard paddle." *American Association of Pharmaceutical Scientists*, 9, pp. 1179-1184(2008).

Bryan, C., "Trends in small-volume dissolution apparatus for low-dose compounds." *Dissolution Technologies*, 2, pp. 19-22(2009).

Scheubel E., Lindenberg M., Beyssac E., "Small volume dissolution testing as a powerful method during pharmaceutical development." *Pharmaceutics*, 2, pp. 351-363(2010).

United States Pharmacopeia 34, "<711> Dissolution", National Formulary 29, pp. 1-8(2011).

Bai G., Armenante, P. M., "Hydrodynamic, mass transfer, and dissolution effects induced by tablet location during dissolution testing." *Journal of pharmaceutical sciences*, 98, pp. 1511-1531(2009).

Bai G., Yimin W., Armenante, P. M., "Velocity profiles and shear strain rate variability in the USP dissolution testing apparatus 2 at different impeller agitation speeds." *International Journal of Pharmaceutics*, 403, pp. 1-14(2011).